POTSDAM-INSTITUT FÜR
KLIMAFOLGENFORSCHUNG

GLOBAL BIOGEOCHEMICAL CYCLES, VOL. 17, NO. 2, 1045, doi:10.1029/2001GB001508, 2003

Simulating past and future dynamics of natural ecosystems in the United States

Dominique Bachelet,[1] Ronald P. Neilson,[2] Thomas Hickler,[3] Raymond J. Drapek,[1,4] James M. Lenihan,[1,4] Martin T. Sykes,[3] Benjamin Smith,[3] Stephen Sitch,[5] and Kirsten Thonicke[5]

Received 17 August 2001; revised 3 April 2002; accepted 21 June 2002; published 15 May 2003.

[1] Simulations of potential vegetation distribution, natural fire frequency, carbon pools, and fluxes are presented for two DGVMs (Dynamic Global Vegetation Models) from the second phase of the Vegetation/Ecosystem Modeling and Analysis Project. Results link vegetation dynamics to biogeochemical cycling for the conterminous United States. Two climate change scenarios were used: a moderately warm scenario from the Hadley Climate Centre and a warmer scenario from the Canadian Climate Center. Both include sulfate aerosols and assume a gradual CO_2 increase. Both DGVMs simulate a reduction of southwestern desert areas, a westward expansion of eastern deciduous forests, and the expansion of forests in the western part of the Pacific Northwest and in north-central California. Both DGVMs predict an increase in total biomass burnt in the next century, with a more pronounced increase under the Canadian scenario. Under the Hadley scenario, both DGVMs simulate increases in total carbon stocks. Under the Canadian scenario, both DGVMs simulate a decrease in live vegetation carbon. We identify similarities in model behavior due to the climate forcing and explain differences by the different structure of the models and their different sensitivity to CO_2. We compare model output with data to enhance our confidence in their ability to simulate potential vegetation distribution and ecosystem processes. We compare changes in the area of drought-induced decreases in vegetation density with a spatial index derived from the Palmer Drought Severity Index to illustrate the ability of the vegetation to cope with water limitations in the future and the role of the CO_2 fertilization effect. *INDEX TERMS:* 1694 Global Change: Instruments and techniques; 1615 Global Change: Biogeochemical processes (4805); 1699 Global Change: General or miscellaneous; 9350 Information Related to Geographic Region: North America; *KEYWORDS:* MC1, LPJ, climate change, fire, carbon, PDSI

Citation: Bachelet, D., R. P. Neilson, T. Hickler, R. J. Drapek, J. M. Lenihan, M. T. Sykes, B. Smith, S. Sitch, and K. Thonicke, Simulating past and future dynamics of natural ecosystems in the United States, *Global Biogeochem. Cycles*, *17*(2), 1045, doi:10.1029/2001GB001508, 2003.

1. Introduction

[2] Vegetation/Ecosystem Modeling and Analysis Project (VEMAP) was an international, collaborative effort supported by several U.S. Global Change Research Program agencies and sponsored by IGBP to conduct an analysis of the potential effects of climate change on ecosystem processes and vegetation distribution within the continental United States [*Schimel et al.*, 1997; *Pan et al.*, 1998]. In phase II of VEMAP, four biogeochemistry models were run with transient historical climate [*Schimel et al.*, 2000] simulating year-to-year variability of the carbon budget from 1980 to 1993. These models simulated changes in the cycling of carbon, water, and nutrients with fixed vegetation types, i.e., allowing no vegetation redistribution through time. However, vegetation dynamics are important when assessing changes in biogeochemical fluxes and therefore, carbon storage. This is particularly true under rapid climate change, where species bioclimatic thresholds may be exceeded, leading to significant changes in vegetation types over large regions [e.g., *Kirilenko and Solomon*, 1998]. A number of dynamic models of vegetation which can predict changes in vegetation and simulate carbon, water, and nutrient cycling at the continental to global scales have been developed [*Foley et al.*, 1996; *Brovkin et al.*, 1997; *Friend et al.*, 1997; *Woodward et al.*, 1998; *Daly et al.*, 2000; *Friend and White*, 2000; *Kucharik et al.*, 2000;

[1]Oregon State University, Corvallis, Oregon, USA.
[2]U.S. Forest Service, Corvallis, Oregon, USA.
[3]Climate Impacts Group, Department of Physical Geography and Ecosystems Analysis, University of Lund, Lund, Sweden.
[4]Now at U.S. Forest Service, Corvallis, Oregon, USA.
[5]Potsdam Institute for Climate Impact Research, Potsdam, Germany.

0886-6236/03/2001GB001508$12.00

Sitch, 2000; *Cramer et al.*, 2001]. Two models of this type were used in phase II of VEMAP to assess the past, present, and future role of dynamically changing the distribution of vegetation types on the biogeochemistry of these biomes while allowing for natural disturbance (wildfires).

[3] In this paper, we compare results from these two models, MC1 [*Daly et al.*, 2000] and LPJ [*Sitch*, 2000], for the period 1895–2100. The models were used to simulate natural vegetation dynamics in response to climatic variations and fire. We discuss differences between model output as they relate to the model structure and process formulation. We also compare results for the historical period (1895–1993) with available data. Model validation is a difficult issue for global or continental models simulating potential vegetation in the absence of limiting nutrients, pests and pathogens, and most of all, any human impacts. To address this issue, we compare model results with *Küchler*'s [1964] potential vegetation map, with net primary production (NPP) data from various sources, and with estimated historical records of biomass consumed and area burnt by wildfires. Moreover, the area of decline in vegetation density simulated by the two models is compared to a Drought Area Index (DAI) derived from the Palmer Drought Severity Index (PDSI) [*Palmer*, 1965] to illustrate the response of the potential vegetation to the spatial distribution of drought periods. *Palmer* [1965] developed a meteorological drought index to objectively measure moisture conditions in the United States. By comparing model output with his index, we emphasize the importance of the simulated CO_2 fertilization effect on the vegetation response to drought stress.

2. Methodology

2.1. Climatic Data

[4] We used two climate change scenarios at a resolution of 0.5° latitude/longitude for the conterminous United States: a moderately warm scenario from the Hadley Climate Centre [*Johns et al.*, 1997; *Mitchell and Johns*, 1997], HADCM2SUL (up to a 2.8°C increase in average annual U.S. temperature in 2100) and a warmer scenario (up to a 5.8°C increase in average annual U.S. temperature in 2100), CGCM1, from the Canadian Climate Center [*Boer et al.*, 1999a, 1999b; *Flato et al.*, 1999]. Both general circulation models (GCMs) include sulfate aerosols and a fully dynamic 3-D ocean. Both transient scenarios start in 1895 and run to the present using observed CO_2 increases [*Schimel et al.*, 2000]. They use IPCC projections of gradual (1% yr^{-1}) future greenhouse gas concentrations (IS92a) [*Kattenberg et al.*, 1996] in the future such that CO_2 atmospheric concentration reaches 712 ppm in year 2100. A spin-up climate time series was created by detrending long-term monthly precipitation and temperature records using a 30-year running average high-pass filter and adjusting the means to the first 15 years of the historical record (1895–1909) (T. G. F. Kittel et al., The VEMAP Phase 2 Bioclimatic Database I: A gridded historical (20th century) climate dataset for modeling ecosystem dynamics across the conterminous United States, submitted to *Climate Research*, 2002). The methodology used to transform the scenarios into a gridded data set and extract future climate trends using an anomaly approach is described elsewhere (T. Kittel et al., unpublished manuscript, 2002). The data were provided by the VEMAP Data Group from the National Center for Atmospheric Research (Boulder, Colorado). There was no direct coupling between the DGVMs and the GCMs and therefore no feedbacks, so that none of the simulated changes in vegetation cover and in carbon fluxes affected the climate.

2.2. Dynamic Vegetation Models

[5] Table 1 summarizes the models similarities and differences.

2.2.1. MC1

[6] MC1 (http://www.fsl.orst.edu/dgvm) is a dynamic vegetation model [*Daly et al.*, 2000; *Bachelet et al.*, 2001a, 2001b, 2000] where the biogeochemical processes are simulated using a modified version of the CENTURY model [*Parton et al.*, 1987, 1993]. A set of biogeography rules based on climatic indices (such as minimum and maximum mean monthly temperatures and growing season precipitation) and leaf area index determines the lifeform (broadleaf or needleleaf, deciduous or evergreen) and the physiological type (C3 or C4 grasses). Vegetation types are defined as a unique combination of trees and grasses in a specific climatic context. This approach was derived from MAPSS, an equilibrium biogeography model [*Neilson*, 1995]. We only show seven vegetation types simulated by MC1 to simplify the analysis of the biogeography results. The correspondence between these vegetation types and the original VEMAP types is described in Table 2. The model is run on a grid using monthly temperature (minimum and maximum), precipitation, vapor pressure, soil depth, soil texture, bulk density, and rock fragment.

[7] The biogeochemistry submodel calculates the biomass of both trees and grasses in each grid cell. MC1, like CENTURY, does not explicitly simulate photosynthesis but uses a maximum potential growth rate that is modified as a function of temperature, soil water availability, self-shading for trees or shading by the overstory canopy for grasses, atmospheric CO_2 concentration, and leaf nitrogen content. Grasses and trees compete for light, water, and nutrients. Plant compartments include leaves, fine and coarse branches, and fine and coarse roots. The model also includes surface and belowground litter and fast, slow, and resistant soil organic matter pools. Both carbon and nitrogen pools are simulated, but nitrogen demand in these simulations is assumed to always be met. The hydrology is a simple "bucket" type with several soil layers and only simulates saturated flow. Soil depth is a spatially variable input to the model and is divided into up to 10 layers. Surface layers are thinner (15 cm) than the deeper thicker (30 cm) horizons that occur below 60 cm in the profile.

[8] Fuel loading in several size classes of both dead and live fuels is estimated from the different carbon pools using lifeform-specific allometric equations [*Lenihan et al.*, 1998]. The moisture content of each dead fuel size class is estimated as a function of antecedent weather conditions averaged over a period of days, the length of which is size-class dependent. The moisture content of each live fuel class is a function of the soil moisture

Table 1. Comparison of the Two Dynamic Vegetation Models[a]

	MC1	LPJ
References	*Daly et al.* [2000], *Bachelet et al.* [2000, 2001a 2001b]	*Sitch* [2000], *Sitch et al.* [2001]
Plant compartments	leaves	leaves
	fine branches, large wood	wood (heartwood and sapwood)
	coarse and fine roots	fine roots
Litter compartments	standing dead, dead fine branches, dead large wood	above and belowground litter
	metabolic and structural surface litter	
	metabolic and structural soil litter	
	dead coarse roots	
Soil compartments	fast, slow, passive soil organic matter	fast and slow soil organic matter
	microbial pool, leachates	
Production	NPP = f(vegc, T, SAW, P, PET, N, CO_2)	GPP = f(I, LAI, T, Wr, PET, CO_2)
	no explicit photosynthesis calculation	photosynthesis using Farquhar approach
		R_A = f(biomass, NPP, T)
CO_2 effect	on NPP, min and max leaf C/N, AET	Increasing intercellular CO_2 thus directly affecting GPP, and indirectly WUE and R_A
PET	*Linacre* [1977] (modified by *Monteith* [1995])	*Jarvis and McNaughton* [1986]
Soil layers	5–10	2
Hydrology	interception, surface runoff, saturated flow (bucket), drainage	Interception, surface runoff, saturated and unsaturated flow (modified bucket), drainage
Nitrogen	nitrogen uptake and allocation	no nitrogen cycle
	nitrogen is assumed to be non limiting	nitrogen is assumed to be non limiting
Fire	process-based (fire behavior is simulated): function of fuel load and arrangement, fuel moisture, air temperature	Function of soil moisture, fuel load (litter only), length of fire season, litter flammability
Competition	for light, water and N	for light and water
Establishment	not simulated	Function of canopy density
Mortality	self-thinning, fire, extreme temperatures, drought	self-thinning, fire, environmental stress

[a]AET, actual evapotranspiration; C/N, carbon to nitrogen ratio; CO_2, carbon dioxide concentration; GPP, gross primary production; I, solar radiation; LAI, leaf area index; N, leaf nitrogen content; NPP, net primary production; P, precipitation; PET, potential evapotranspiration; R_A, autotrophic growth respiration; SAW, soil available water; T, (air) temperature; vegc, total live vegetation carbon; Wr, root zone water supply; WUE, water use efficiency.

content to a specific depth in the profile. Fuel moisture and the distribution of the total fuel load among the different size classes determine potential fire behavior using the *Rothermel* [1972] fire spread equations. Thresholds of potential fire spread, fine fuel flammability, and coarse woody fuel moisture are used to trigger the occurrence of a simulated fire event, given a constraint of just one fire event per year. Simulated fire intensity and the vertical structure of the vegetation interact to determine transitions from surface to crown fire. The impact of a fire event is simulated in terms of the fraction of the cell burnt and the mortality and consumption of carbon within the area burnt. The area burnt depends on the current fire return interval simulated for the cell, the amount of time elapsed since the pixel area last burnt, and the simulated rate of fire spread. Live carbon mortal-

Table 2. Correspondence Between the DGVM Vegetation Types and VEMAP Types

Aggregated Vegetation Types	VEMAP Vegetation Types
1. Coniferous forests	2. boreal coniferous forest
	3. temperate maritime coniferous forest
	4. temperate continental coniferous forest
2. Winter deciduous forests	7. temperate deciduous forest
3. Mixed conifer-broadleaved forests	5. cool temperate mixed forest
	6. warm temperate/subtropical mixed forest
4. Broadleaved evergreen drought-deciduous forests	8. tropical deciduous forest
	9. tropical evergreen forest
5. Savannas and woodlands	10. temperate mixed xeromorphic woodland
	11. Temperate conifer xeromorphic woodland
	12. tropical thorn woodland
	13. Temperate deciduous savanna
	14. warm temperate/subtropical mixed savanna
	15. Temperate conifer savanna
	16. tropical deciduous savanna
6. Grasslands and shrublands	1. tundra
	17. C_3 grasslands
	18. C_4 grasslands
	19. Mediterranean shrubland
	20. temperate arid shrubland
7. Deserts	21. subtropical arid shrubland

ity and consumption are functions of the simulated fireline intensity and lifeform-specific morphology (i.e., crown height, crown length, and bark thickness). Dead fuel consumption is simulated using functions of fuel moisture that are fuel-class specific.

2.2.2. LPJ

[9] The Lund-Potsdam-Jena (LPJ) DGVM [*Sitch et al.*, 2003; *Smith et al.*, 2001] is one of a family of models derived from the BIOME3 terrestrial biosphere model [*Haxeltine and Prentice*, 1996b]. Vegetation in the model is characterized by combinations of 10 plant functional types (PFTs) with different physiological (C3, C4 photosynthesis), phenological (deciduous, evergreen), and physiognomic (tree, grass) attributes. Combinations of PFTs were grouped for this project into seven aggregated vegetation types that correspond to combinations of the original VEMAP vegetation types (Table 2). The model is run on a grid using soil texture, monthly temperature, precipitation, and percentage of maximum sunshine. Bioclimatic limits determine which PFT can establish and survive under current conditions, while individual growth, population dynamics (including competition between PFTs), and disturbance by fire partition the grid cell among the PFTs present and "bare ground." The fractional coverage of each PFT is derived from the density of average individuals in the grid cell, their summed leaf area, and the extent of their canopy. Annual plant establishment, in terms of additional PFT individuals, depends on the fraction of bare ground available for seedlings to successfully establish and on the number of woody PFTs already present.

[10] The state variables for an average individual of a PFT are leaf, sapwood, heartwood, and fine root biomass. Allometric relationships allow height, stem diameter, and crown area to be derived from the fundamental state variables. Each compartment is assigned a C:N ratio and a turnover time. Maintenance and growth respiration are calculated daily for each PFT based on tissue biomass, C:N ratio, and environmental conditions. Annual net primary production (NPP) is allocated to the leaf, sapwood, and fine root compartments to satisfy the prescribed allometric relationships. Moisture stress can affect relative allocation to roots versus other compartments. Photosynthesis is calculated at midmonth for each PFT based on its fractional coverage, its current phenology, and the water availability in the rooting zone. A modified Farquhar approach [*Haxeltine and Prentice*, 1996a, 1996b] assumes optimal allocation of leaf nitrogen though vegetation canopies and throughout the season, and includes a dynamic feedback between photosynthesis and soil hydrology through canopy conductance.

[11] The two-layer soil water balance submodel is based on the approach of *Haxeltine and Prentice* [1996b] and *Haxeltine et al.* [1996]. The moisture status of each soil layer, expressed as a fraction of its water holding capacity, is updated daily based on plant uptake, percolation from the upper to the lower layer, and water holding capacity that is soil texture dependent.

[12] Mortality corresponds to an annual reduction in the density of PFT average individuals. It includes a stress component, the inverse of PFT vigor, and a self-thinning component that increases as the grid cell approaches 100% cover by woody PFT's. Light competition favors woody over grass PFTs.

[13] Litter is produced annually as a result of leaf and root turnover and enters aboveground and belowground litter pools, respectively. Daily decomposition in the litter pools results in respiration to the atmosphere and transfer of the remaining carbon to the soil pools for further decomposition. Litter pools are also augmented by biomass killed by background and stress mortality, and by fire disturbance.

[14] Disturbance by fire is imposed as a reduction in density of PFT average individuals. The fraction of a given grid cell affected by fire each year is calculated based on the length of the fire season and the fuel load. The LPJ fire module Glob-FIRM [*Thonicke et al.*, 2001] uses the simulated moisture of the upper soil layer as a surrogate for fine fuel moisture and a single threshold of litter carbon to account for fuel loading. The probability of at least one fire occurring in a day and in a grid cell is a function of soil moisture and the PFT-specific moisture of extinction, a threshold above which fire does not spread. The cumulative probability of fire occurrence throughout the year estimates the length of the fire season. If the threshold of litter loading (200 g C m^{-2}) is met, the length of the fire season determines the fraction of the cell area burnt annually. The fraction of the different PFTs killed depends on the fraction of the cell burnt and prescribed PFT fire resistances.

3. Protocol to Run the DGVMs

3.1. Protocol to Run MC1

3.1.1. Equilibrium Mode: Initialization Phase

[15] The MAPSS equilibrium biogeography model [*Neilson*, 1995] is first run (stand-alone mode) with mean 1895–1994 monthly climate data and soil information to produce an initial potential vegetation map. MC1 biogeochemistry module is then initialized with this vegetation map and run with the same mean climate to calculate corresponding initial carbon and nitrogen pools. The run terminates when the slow soil organic matter pool reaches steady state which may require up to 3000 simulation years for certain vegetation types [*Daly et al.*, 2000]. This phase corresponds to the initialization of all MC1 variables. Because MC1's fire module cannot be run meaningfully on a mean climate, fire frequency is prescribed for each vegetation type in this equilibrium phase.

3.1.2. Transient Mode With Spin-Up Phase

[16] Once the slow-turnover soil carbon pools have equilibrated, MC1 is run in transient mode using a climate time series. This time series is created by linking the spin-up climate time series (100 years) provided by NCAR and the transient climate of interest (historical followed by future, 200 years total). The MC1 fire module is only used in transient mode and requires the spin-up phase to attain a spatially variable fire frequency.

3.2. Protocol to Run LPJ

[17] The simulation starts from bare ground and the model is spun up for 1000 years (10 times the 100 year spin-up climate time series provided by NCAR) until the vegetation

reaches equilibrium. Soil organic matter pools are the slowest ecosystem component to reach equilibrium. However, with vegetation cover at equilibrium, the annual litter input to the soil is more or less constant which allows for the analytical solution of differential equations relating litter inputs to soil carbon pool sizes (in MC1, which includes nutrient cycling, final pool sizes cannot be derived analytically). Once equilibrium has been reached, LPJ is run with the historical climate time series and the future scenarios. Fire is simulated dynamically during the entire simulation including spin-up.

4. Definition and Calculation of PDSI and Stress Area

4.1. PDSI and DAI

[18] A monthly PDSI [*Palmer*, 1965] based on VEMAP monthly temperature and precipitation data, as well as on soil-water holding capacity, was obtained from NCAR (D. Yates and VEMAP Data Group, unpublished data set, 1995). We calculated the average annual value for PDSI and the annual drought area index (DAI) representing the area of the conterminous United States where the annual PDSI is less than zero for any given year [*Diaz*, 1983].

4.2. Stress Area Index or SAI

[19] Large-scale vegetation decline is commonly caused by drought which follows either a reduction in precipitation, or an increase in evaporative demand (higher temperatures), or both. Our analysis is similar to the spatial mapping of the PDSI [*Palmer*, 1965]. The objective is to relate regional patterns of drought or vegetation stress to large-scale atmospheric circulation changes on both short and long timescales [e.g., *Nigam et al.*, 1999].

[20] We first calculated the long-term average live vegetation carbon simulated for the spin-up climate time series (detrended historical climate) described earlier. We then calculated, for each year of the simulation and for each grid cell, the difference between the current year simulated live vegetation carbon and that from the spin-up period. The fraction of the U.S. lands and forested areas where that difference was negative (live vegetation $\text{carbon}_{\text{year}}$ < live vegetation $\text{carbon}_{\text{spin-up average}}$) was defined as the stress area index or SAI.

[21] We expect the SAIs to follow DAI under constant CO_2, but under increasing CO_2, we expect SAI to be lower than DAI due to an increase in plant water use efficiency induced by CO_2.

5. Results

5.1. Potential Vegetation Distribution

5.1.1. Historical Conditions (1895–1993)

[22] We compared the vegetation distribution simulated by both models in 1900 and in 1990 to *Küchler*'s [1964] potential vegetation map (Figure 1). Küchler's work remains the best available at the continental scale describing U.S. potential vegetation for the middle of the twentieth century. Both models capture the broad patterns of vegetation distribution across the United States including the eastern deciduous forests, the western coniferous forests, the central Great Plains, and the Desert Southwest. However, there are several areas of disagreement between model results and Küchler's map: MC1 simulates evergreen forests in northern Maine, deciduous forests in the Carolinas, and grasslands occupying the Prairie Peninsula region south of the Great Lakes. MC1 also simulates areas of savannas bordering the western coniferous forest areas in the western states. Both models fail to simulate the extensive deserts of southern New Mexico and western Texas, but MC1 simulates wider ranging than expected deserts in Utah. LPJ simulates evergreen forests from the Atlantic coast of the Carolinas to Oklahoma, and savannas and woodlands extending into the northern Great Plains region. The percent agreement table (Table 3) quantifies those differences. The greatest lack of agreement between the model simulations and Küchler's map occurs in savannas. Savannas represent ecotones between grasslands and forests. If either the limits of the forests or of the grasslands are misplaced, the location of the savannas is misrepresented and statistical accuracy becomes poor. Basic statistics cannot accurately measure the topology of the spatial relationships between biomes and ecotones. In the west, woodlands correspond to small patches of a few pixels at the resolution of our simulation and are difficult to capture to exactly match the location defined in Küchler's. The total area represented by woodlands can be close to the actual measurement but the location missed by a short distance. Again, basic statistics will not capture the fact that woodlands are represented, if not in the correct location, but will only focus on the spatial accuracy. Some of the mismatch can be partially explained by the role of fire in the models. There is a continuous shift between savannas and grasslands in MC1 as the woody component disappears after each fire occurrence. In drought-prone areas such as the Great Plains where fire return intervals are high, this shift can be particularly frequent.

5.1.2. Future Conditions (1994–2100)

[23] Under HADCM2SUL, MC1 simulates the loss of the prairie peninsula area by 2030 when mixed and coniferous forests invade the historical savannas (Figure 2a). It also simulates the expansion of the eastern forests west of the Mississippi, particularly during the second half of the 21st century (Figure 3a). The same results were obtained whether CO_2 was held constant or not (Figures 2a, 2c, 3a, and 3c). LPJ does not simulate the prairie peninsula as a savanna and open-woodland area during the twentieth century (Figure 1). It predicts the expansion of the eastern deciduous forest westward and northward, in a more pronounced fashion when atmospheric CO_2 is increasing (Figures 2b and 2d, 3b and 3f). In both MC1 and LPJ simulations, desert areas of the southwest become greatly reduced by the end of the 21st century (Figure 3), especially under elevated CO_2 (Figures 3a and 3b) where they are replaced mostly by grasslands. Concurrently, savannas and woodlands of north-central California are replaced by forests (Figures 3a, 3b, 3e, and 3f) and savannas expand in the interior west.

[24] Under CGCM1, MC1 simulates the loss of the prairie peninsula woodlands to mixed and deciduous forests

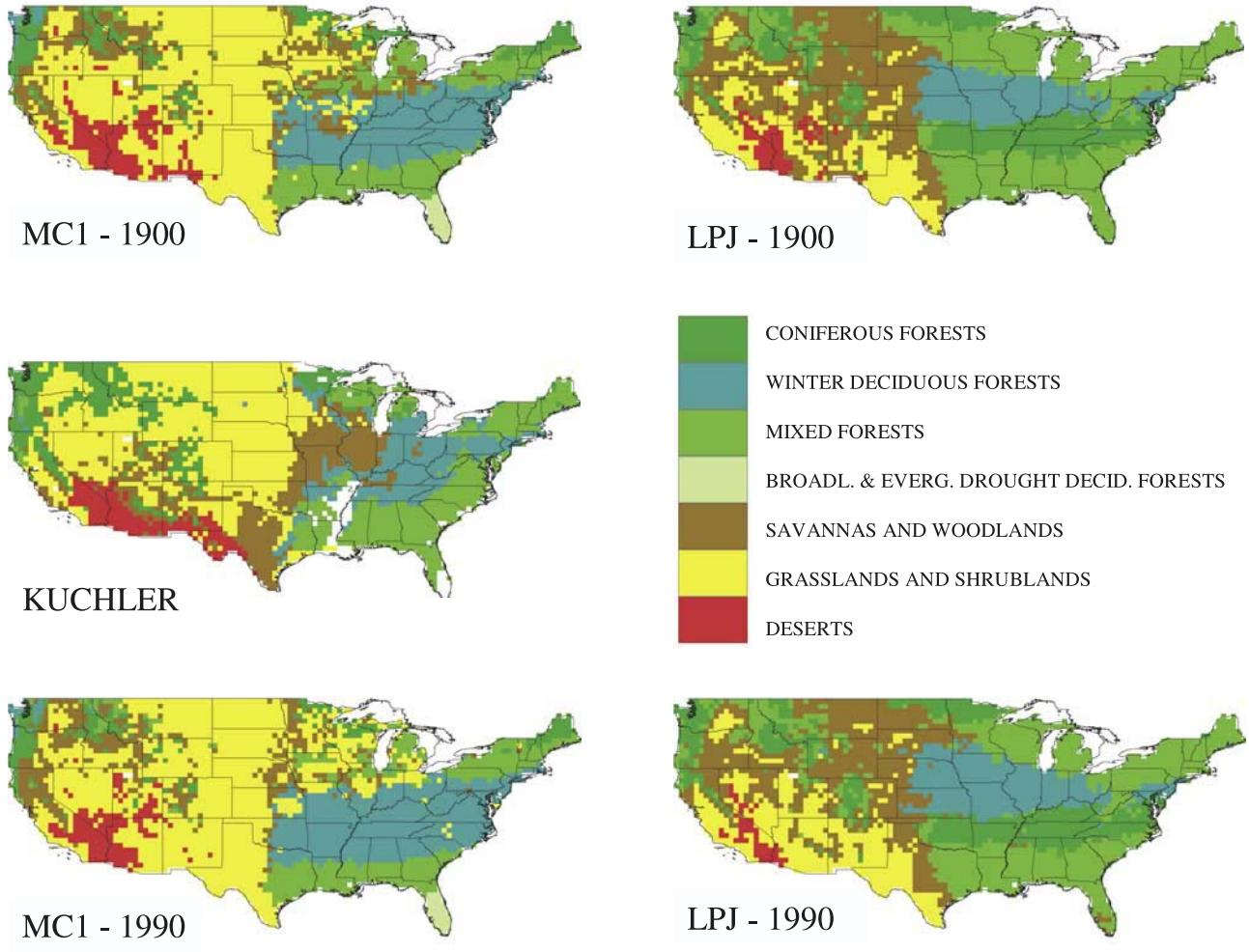

Figure 1. Distribution of aggregated vegetation classes simulated by MC1 and LPJ in 1900 and 1990 and mapped by *Küchler* [1964]. Models assume a continuous increase in the atmospheric CO_2 concentration from 295 ppm in 1895 to 354 ppm in 1990.

(Figures 2e and 2g, 3e and 3g). It simulates the expansion of the broad-leaved evergreen-drought deciduous forests from Florida where it already exists in 1900 to eastern Texas, Louisiana, and the southern portions of Mississippi, Alabama, and Georgia (Figures 3b and 3d). Both models agree about the loss of coniferous forests in the Great Lakes area and the great reduction in desert areas of the Southwest (Figures 3e and 3f). Both models forecast the expansion of forests in the western part of the Pacific Northwest and in north-central California (Figures 2e and 2g). MC1 simulates a large area of grasslands north of Louisiana caused by droughts occurring around 2030 (Figures 3b and 3d), while LPJ simulates a large area of drought-caused savannas in Mississippi and Alabama by 2095 (Figures 3f and 3h).

5.2. Carbon Budget

5.2.1. Carbon Fluxes

[25] Since the changes in total carbon storage vary considerably from year to year, we used a 10-year running average value to document the carbon source and sink strength of the conterminous United States through time (Figure 4). Both models agree that, during the drought of the 1930s, the United States had become a carbon source of about 0.3 Pg yr^{-1}. LPJ simulates another source of about

Table 3. Percentage Agreement Between the Vegetation Maps Simulated by LPJ and MC1 for 1900 and 1990 and *Küchler*'s [1964] Published Map of Potential Vegetation (1964)[a]

Küchler	MC1 1900, %	LPJ 1900, %	MC1 1990, %	LPJ 1990, %
Coniferous forests (387)	43	44	29	45
Deciduous forests (368)	62	27	68	29
Mixed forests (562)	48	78	47	78
Savannas and woodlands (512)	10	24	10	21
Grasslands and shrublands (1175)	73	19	75	22
Deserts (164)	71	37	53	23
Overall	51	38	47	36

[a]In parentheses are the number of pixels associated with each aggregated vegetation type in the digital Küchler map.

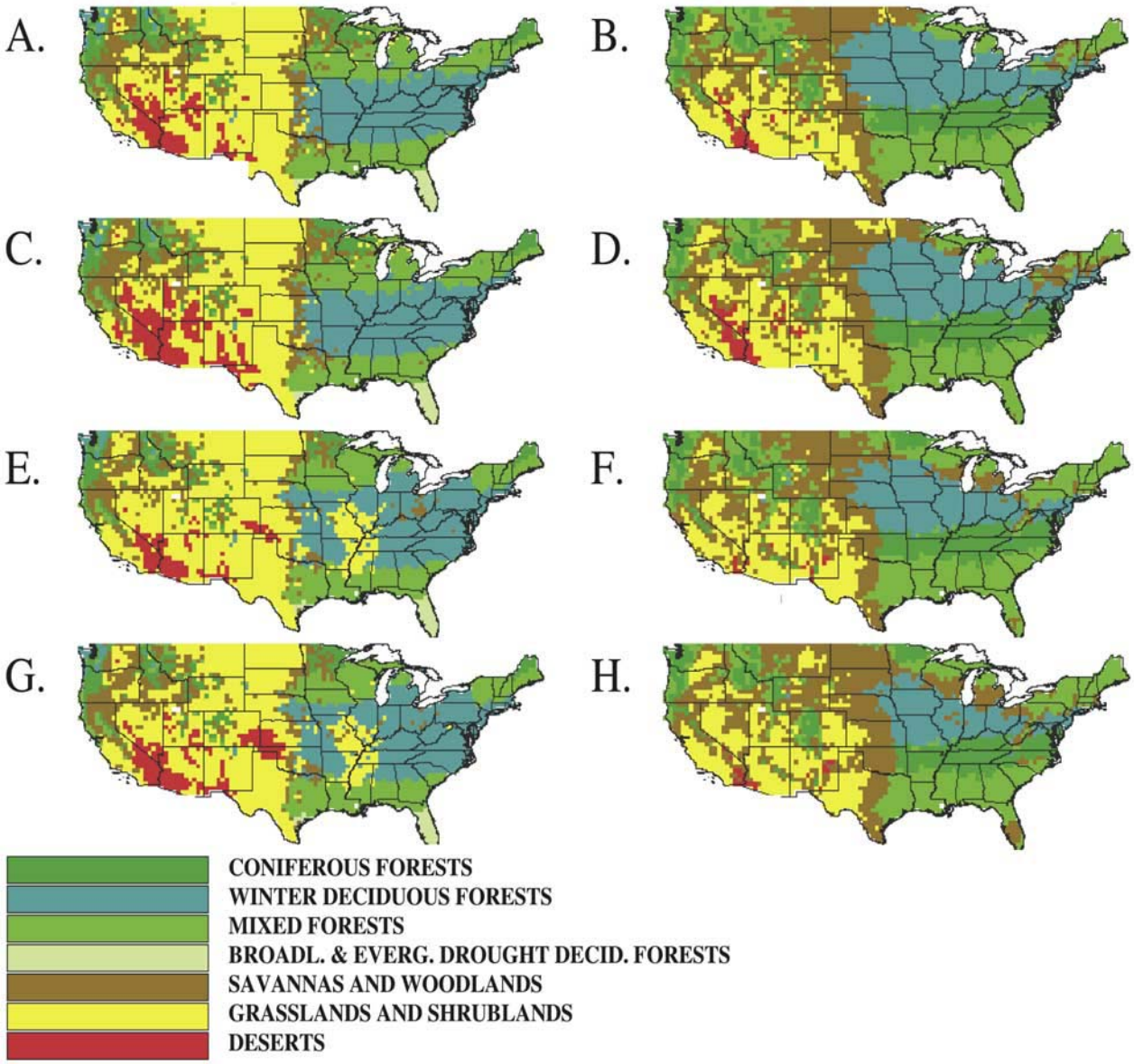

Figure 2. Distribution of aggregated vegetation classes simulated by (left column) MC1 and (right column) LPJ in 2030 under (a–d) HADCM2SUL and (e–h) CGCM1. Models assume either a continuous increase in the atmospheric CO_2 concentration from 295 ppm in 1895 to 712 ppm in 2100 (Figures 2a, 2b, 2e, and 2f), or a constant atmospheric CO_2 concentration of 295 ppm from 1895 to 2100 (Figures 2c, 2d, 2g, and 2h).

0.2 Pg yr^{-1} during the drought of the 1950s. MC1 simulates a source around 1988, which was a big fire year in the western United States and the upper Midwest (Prairie Peninsula area). During the 21st century, MC1 projects mostly an increase in the U.S. sink size under HADCM2-SUL except between about 2055 until 2070 when it simulates a source of about 0.4 Pg C yr^{-1}. Under CGCM1, MC1 projects mostly an increase in the U.S. source size particularly in the first half of the 21st century (up to 0.6 Pg C yr^{-1} by 2040) except shortly before 2050 and at the end of the century when it simulates a small sink (0.15–0.25 Pg C yr^{-1}). Under constant CO_2, LPJ simulates the United States as a continuous source in the 21st century under both climate change scenarios, most pronounced under CGCM1 (0.5 Pg C yr^{-1}). When atmospheric CO_2 concentration is increasing, LPJ simulates mostly a carbon sink of about 0.2 Pg C yr^{-1} over the United States under HADCM2SUL, with dynamics close to those of MC1. Under CGCM1, LPJ simulates a 0.2 Pg C yr^{-1} source during the second half of the 21st century but either a source (2020s and 2040s) or a sink (2030s and 2060s) earlier on.

5.2.2. Carbon Pools

[26] The dynamics of the two model simulations are similar under the moderately warm HADCM2SUL scenario but strikingly different under CGCM1 (Figure 5). Total carbon storage remains stable for both models (135 Pg for

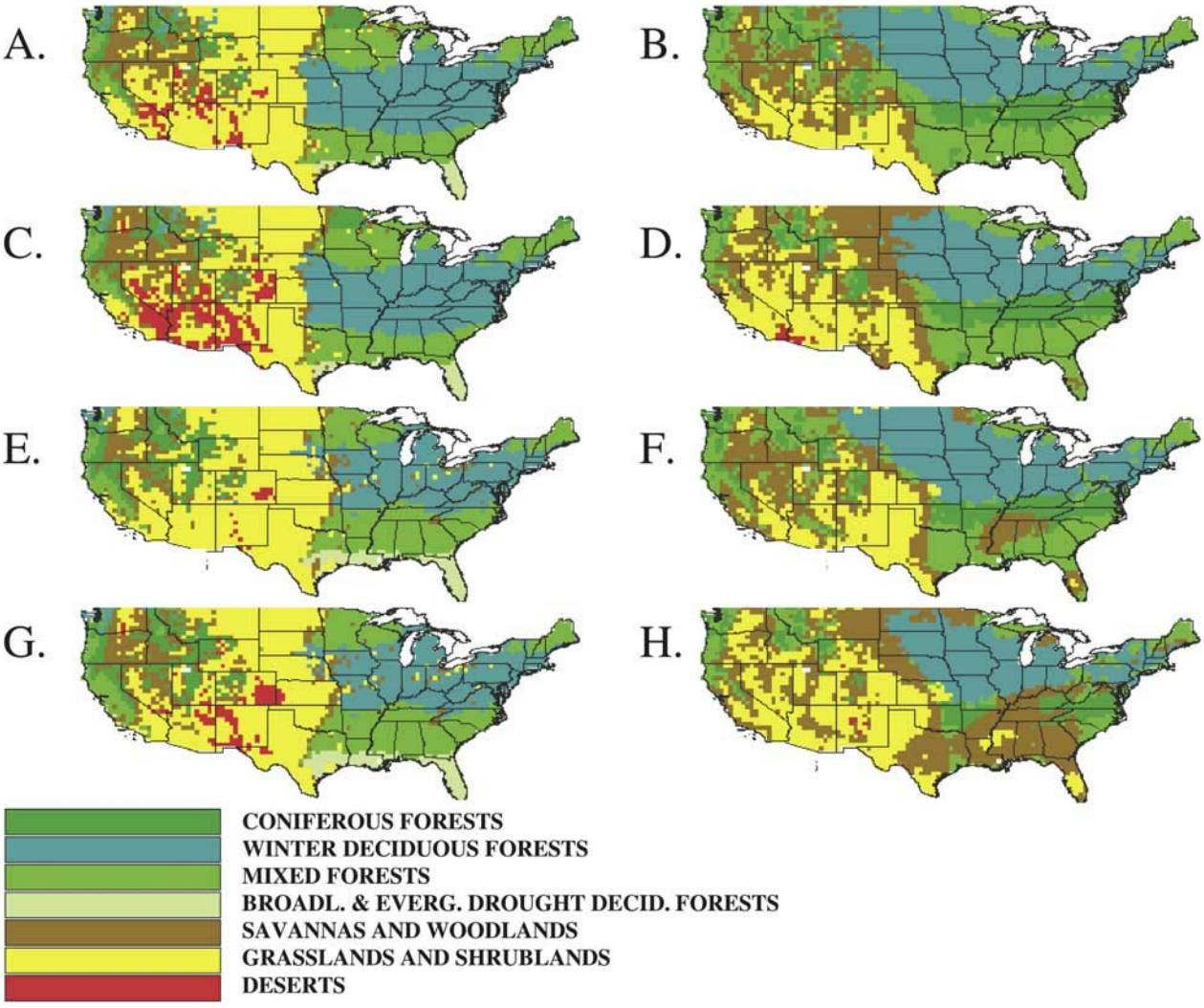

Figure 3. Distribution of aggregated vegetation classes simulated by (left column) MC1 and (right column) LPJ in 2095 under (a–d) HADCM2SUL and (e–h) CGCM1. Models assume either a continuous increase in the atmospheric CO_2 concentration from 295ppm in 1895 to 712 ppm in 2100 (Figures 2a, 2b, 2e, and 2f), or a constant atmospheric CO_2 concentration of 295 ppm from 1895 to 2100 (Figures 2c, 2d, 2g, and 2h).

MC1, 175 Pg for LPJ) in the early part of the twentieth century (Figures 5a and 5b). In the 1950s, total carbon storage begins to increase for MC1 with both constant and elevated atmospheric CO_2 concentrations, but only under increasing CO_2 concentration for LPJ. Under CGCM1, MC1 simulates a decrease in total C storage below historical levels with partial recovery under elevated CO_2. When CO_2 is held constant, LPJ simulates a continuous decrease in C storage throughout the 21st century. Under HADCM2SUL, MC1 simulates future increases in live vegetation carbon pools (from 0.028 to 0.037 Pg) even when atmospheric CO_2 concentration is held constant, but simulates an overall decrease under CGCM1 (Figure 5c). LPJ, on the other hand, simulates an increase in live vegetation carbon pools (from 0.053 to 0.065 Pg under HADCM2SUL and 0.070 Pg under CGCM1) under both scenarios when CO_2 increases, but it simulates a decrease (down to 0.042 Pg under CGCM1 and down to 0.050 Pg under HADCM2SUL) when CO_2 concentration is held constant (Figure 5d).

[27] Soil carbon pool dynamics (Figures 5e and 5f) follow a similar but more pronounced pattern. When atmospheric CO_2 concentration is held constant, LPJ simulates a decrease in soil carbon at the beginning of the 21st century under both scenarios (from 0.123 Pg in the second half of the twentieth century to 0.100 Pg under CGCM1 and 0.105 Pg under HADCM2SUL). But when CO_2 increases, LPJ first simulates a small increase (from 0.124 to 0.129 Pg) in soil carbon during the first half of the 21st century followed by a small decrease under HADCM2SUL and a sharper decrease (to 0.120 Pg) under CGCM1 below historical levels. MC1 simulates a small increase in soil carbon in the second half of the twentieth century followed by a decline under CGCM1, more pronounced when CO_2 concentration is held constant. Under HADCM2SUL, when CO_2 concentration increases, soil carbon increases from

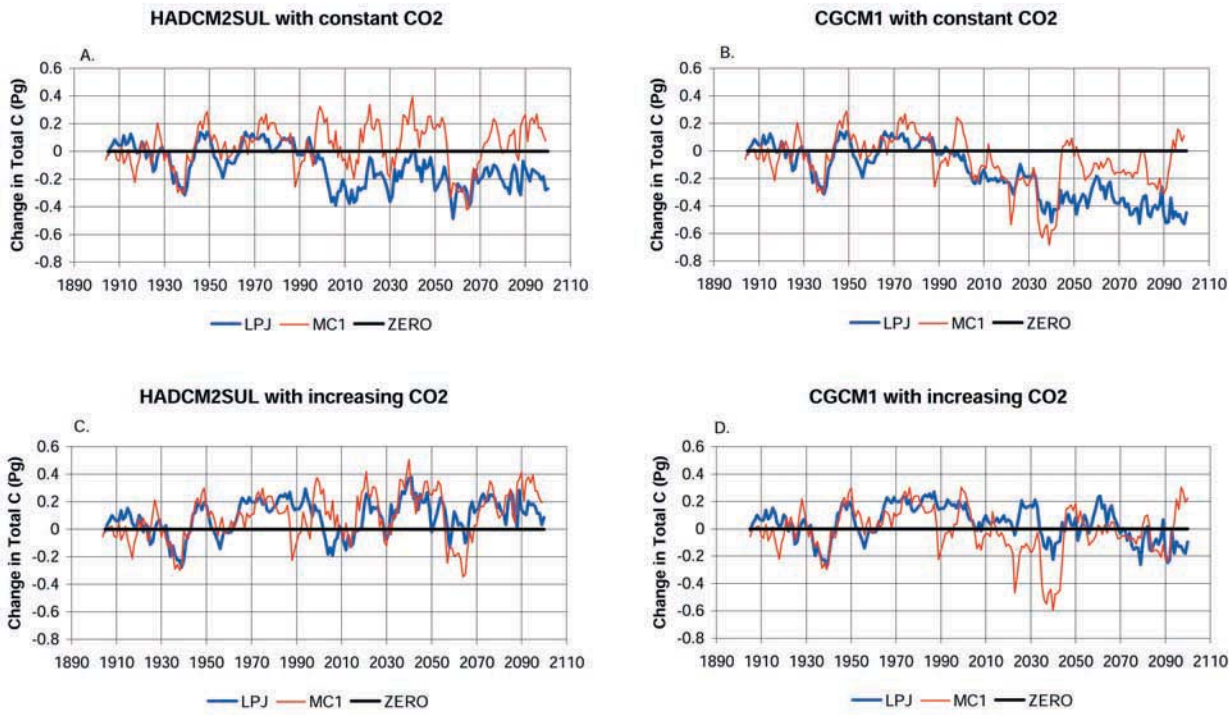

Figure 4. Change in total carbon storage simulated by MC1 and LPJ from 1895 to 2100 for HADCM2SUL and CGCM1 climate change scenarios. Models assume either a constant atmospheric CO_2 concentration of 295 ppm or a continuous increase in the atmospheric CO_2 concentration from 295 ppm in 1895 to 712 ppm in 2100.

historical levels to 0.115 Pg. When CO_2 concentration is held constant, soil carbon only slightly increases until the middle of the 21st century when it collapses back to historical levels. In both cases, there is an increasing trend between 2080 and the end of the century.

[28] There is a fundamental difference in the models' sensitivity to the two climate scenarios and the two CO_2 concentrations (Figure 5). For MC1, the difference between the climate scenarios is always greater than the difference between the CO_2 scenarios. The reverse is true for LPJ. In LPJ, net primary production enhancement due to the atmospheric enrichment in CO_2 is enough to compensate for the drier conditions until it reaches a threshold beyond which water availability becomes the limiting factor. In MC1, environmental conditions regulate net primary production further than the CO_2 effect. To better compare the two model responses to CO_2, we plotted the changes in live vegetation and soil carbon against the increasing atmospheric CO_2 concentration and normalized the carbon pool sizes (Figure 6). The drought impact of CGCM1 on the size of the carbon pools is significant for both models, but the CO_2 effect in LPJ allows the model to continue to simulate an increase in biomass while MC1 simulates a sharp decrease.

5.2.3. Effect of Fire

[29] The MC1 fire module simulates on average 73% more area burnt annually than does LPJ during the historical portion of the simulations (Figure 7). *Leenhouts* [1998] provided an independent estimate of the range of annual acreage burnt under presettlement conditions (Table 4a). The corresponding MC1 estimate is just below the lower end of Leenhouts' estimate, while the LPJ estimate is substantially lower. MC1 and LPJ produce a similar level of variation in area burnt throughout the historical period (coefficients of variation are 36% and 31%, respectively). However, MC1 simulates a greater number of small size (<30% pixel area burnt) and large size (>80% pixel area burnt) areas burnt than LPJ (Figure 7) under both historical and future climate conditions.

[30] Both MC1 and LPJ simulate only small increases in average annual acreage burnt under the HADCM2SUL scenario (increases of 4% and 6%, respectively), but simulate substantially larger increases under the CGCM1 scenario (increases of 22% and 31%, respectively). MC1 continues to burn more acreage than LPJ under both future scenarios, and the variability in area burnt simulated by both models during the future scenario periods is comparable to that during the historical period. MC1 simulates increase in the number of medium to large fire events under CGCM1. LPJ only simulates an increase in very large fire events (>70% pixel area burnt) under CGCM1. While LPJ simulates an increase in small to medium-size fire frequency under HADCM2SUL, MC1 simulates a decrease in medium to large size fires (>50% pixel area burnt) under HADCM2SUL.

[31] Despite burning more area than LPJ, MC1 simulates on average 60% less annual biomass consumed by fire than LPJ during the historical period (Figure 8, Table 4b). The

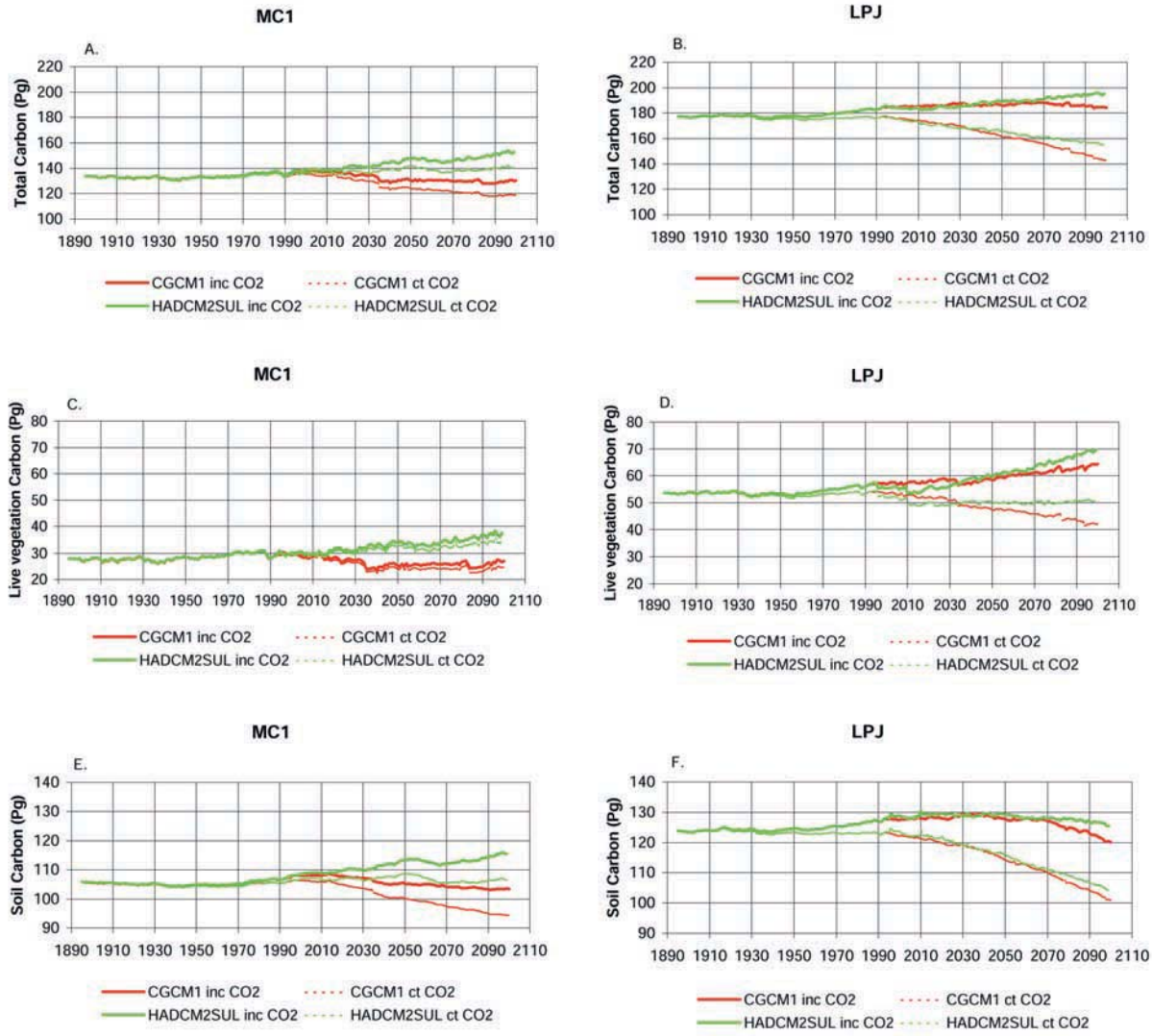

Figure 5. (a, b) Total vegetation carbon, (c, d) live vegetation, and (e, f) soil carbon simulated by MC1 and LPJ from 1895 to 2100 under HADCM2SUL and CGCM1 climate change scenarios. Models assume either a constant atmospheric CO_2 concentration of 295 ppm (ct. CO_2) or a continuous increase in the atmospheric CO_2 concentration (inc. CO_2) from 295 ppm in 1895 to 712 ppm in 2100.

MC1 and LPJ estimates of average annual biomass consumed by fire fall in the middle and at the end of the range of *Leenhouts*' [1998] estimate, respectively. The trend of biomass consumed by fire simulated by MC1 shows much greater variability than the LPJ simulation for the historical period (coefficients of variation are 68% and 19%, respectively). The difference is most evident in the large peaks of consumption exhibited by the MC1 simulation that are largely absent in the LPJ simulation (Figure 8). The timing of the peaks correspond to documented periods of extreme drought and very large fire events in the United States (e.g., 1910, the 1930s, 1988) and match some of the large variations in C storage (Figures 4 and 8). Both MC1 and LPJ simulate only small changes in average annual biomass consumed by fire under the HADCM2SUL scenario (+11% and −1%, respectively), but simulate significant increases under the CGCM1 scenario (increases of 36% and 22%, respectively). LPJ continues to consume substantially more biomass than MC1 under both future scenarios. The variability in biomass consumed by fire simulated by each model for the future scenarios is comparable to that during the historical period, with one exception. The variability simulated by MC1 under the HADCM2SUL scenario is significantly lower than for the historical period (coefficients of variation are 68% for the historical period and 38% for the HADCM2SUL scenario).

5.3. Simulated Area of Vegetation Decline in the United States: Comparison With DAI

5.3.1. DAI Dynamics

[32] We compared the DAI calculated directly from the VEMAP climate data with the SAI or fractional area of U.S. land that underwent a decline in vegetation density simulated by both models. Since both DAI and SAI vary considerably

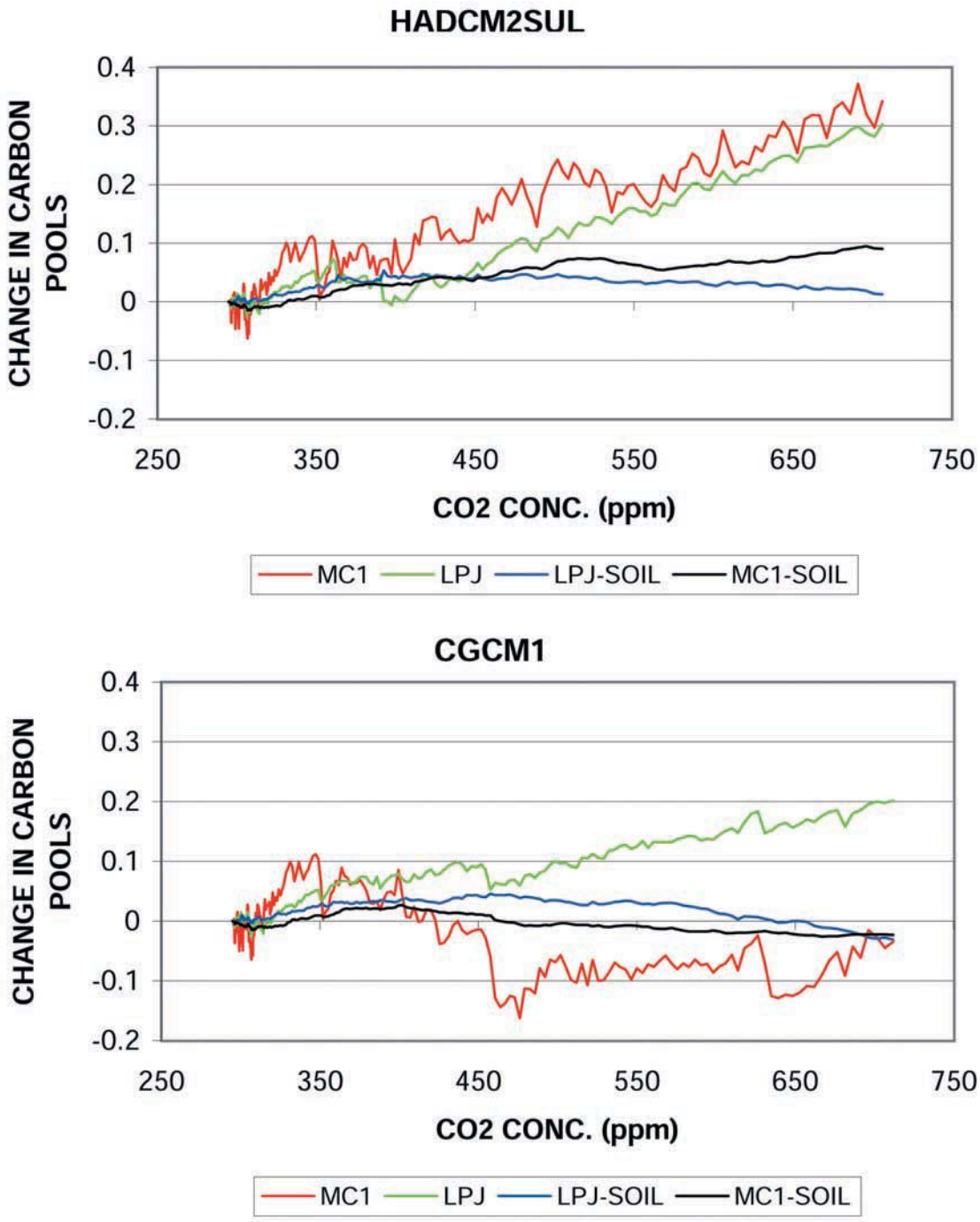

Figure 6. Live vegetation and soil carbon simulated by the two DGVMs from 1895 to 2100, under HADCM2SUL and CGCM1, plotted against atmospheric CO_2 concentration. Carbon pools were normalized to 1.0 to facilitate the comparison between the model responses to CO_2. Models assume a continuous increase in the atmospheric CO_2 concentration from 295 ppm in 1895 to 712 ppm in 2100.

from year to year (Figure 9a), we used a 10-year average DAI and SAI to look at long-term trends such as large historical droughts (Figure 9b). The 1930s drought stands out as the most severe of the twentieth century and affects over 60% of the U.S. land surface between 1933 and 1940. The drought of the 1950s also stands out, but by the mid-1960s DAI starts decreasing from a high around 60% to a low around 45% by the mid-1980s. This decline can be linked to an observed increase in the precipitation regime over North America and a shift from 3 decades of cooling to persistent warming [*Karl*, 1998]. Because CGCM1 is warmer and drier, it affects a larger fraction of the country, and over 70% of the U.S. lands have a negative PDSI in the 21st century. Under HADCM2SUL, only about 50% of the country is under

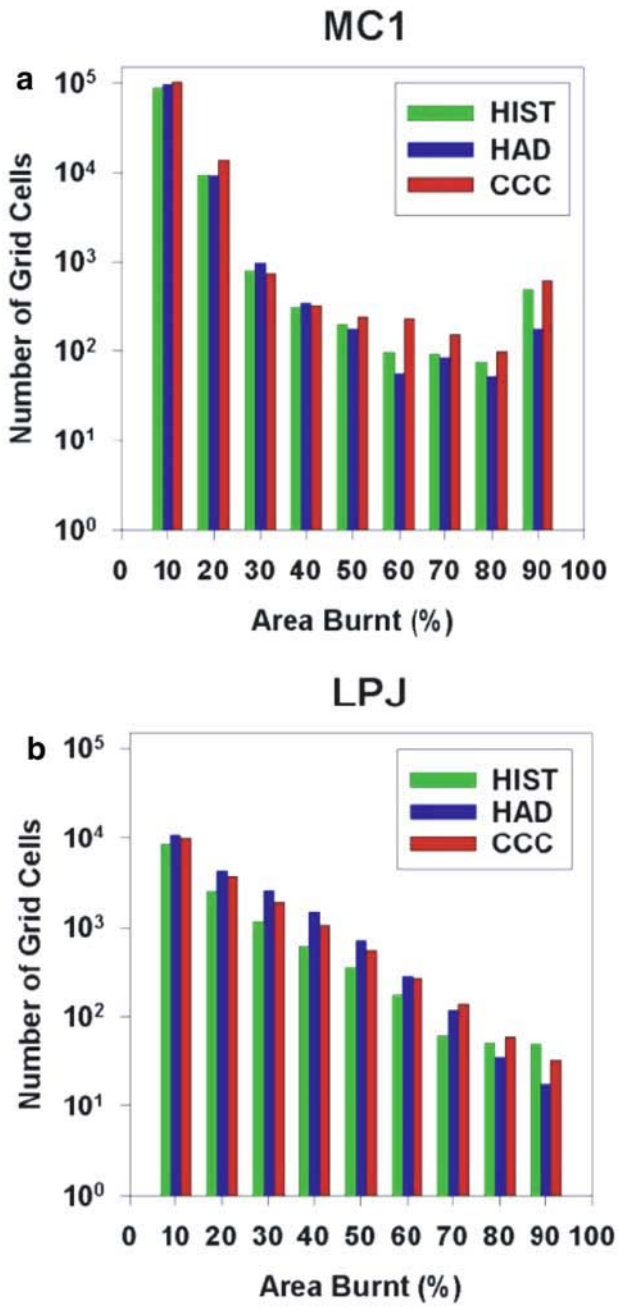

Figure 7. Frequency distribution of the pixels sustaining wildfires as simulated by (a) MC1 and (b) LPJ, for historical conditions (1895–1994) and for HADCM2SUL and CGCM1 climate change scenarios (1995–2100).

stress until about 2070, when the area under stress decreases to a low of 35% at the end of the 21st century.

5.3.2. SAI Dynamics

[33] Both models simulate similar dynamics of U.S. drought stress area under historical conditions (Figures 10 and 11) and follow the DAI fairly closely. When CO_2 is allowed to increase, both models simulate a smaller area under stress in the 1980s than the DAI and do not show the early 1990s small drought period that DAI simulates as affecting 50% of the country. *Changnon*'s [1989] estimates (based on the PDSI) that about 40% of the United States was under severe to extreme drought in 1988 alone. Both models simulate a plant CO_2 response that the DAI does not include that mitigates the drought impacts.

[34] When CO_2 is held constant in the future, the two models agree fairly well under both scenarios and follow DAI relatively closely with up to 70% of the U.S. lands under drought stress under CGCM1 (Figure 11b). Both models simulate less drought impact than DAI between 1990 and 2020. When CO_2 is increasing, the models strongly differ under CGCM1 (Figure 11). LPJ simulates about 25% of the U.S. lands under drought stress from 2045 until the end of the 21st century, while MC1 follows more closely the DAI, reaching 60% of drought stress area by 2095. The CO_2 effect in LPJ compensates for the drought effect, while it does not in MC1. Under HADCM2SUL, both models agree closely, underestimating the area under stress (20%) in comparison with the DAI (35–50%). There is an overall continuous decline in the stress area between 2020 and 2095 that implies that increased precipitation associated with moderate warming is favoring plant growth (Figure 10b). Unlike LPJ, there was little difference in MC1 output between the constant and increasing CO_2 scenarios illustrating again the difference in sensitivity to CO_2 between the two DGVMs and the importance of the simulated positive effects CO_2 on water use efficiency in LPJ.

6. Discussion

[35] It is remarkable that two models with such different structures as MC1 and LPJ consistently simulated similar overall trends in vegetation distribution and carbon cycling throughout the conterminous United States. Before summarizing the various scientific conclusions emerging from this model comparison, it is necessary to note the various limitations that are inherent to such modeling exercises. The quality of the climatic input data, the structure and inherent simplifying assumptions the models include, and the scarcity of validation data sets all constrained this project. However, the differences between the simulations of plant sensitivity to CO_2 and of plant responses to fire emphasized important scientific issues that remain important subjects for discussion. The lack of data documenting the actual response of mature forests to increasing atmospheric CO_2 and the scarcity of fine-scale environmental data to test the fire models are two such examples. The differences in design of their fire modules and productivity response to CO_2 are also the trademarks of these two models, which have been designed with the ability to simulate vegetation

Table 4a. Average Area Burnt in the Conterminous United States: Simulated Versus Observed[a]

	Average Area Burnt, 10^6 ha		
	LPJ	MC1	*Leenhouts* [1998]
1895–1995	19.1	33.2	35–86
1994–2100: HADCM2SUL	20.2	34.4	
1994–2100: CGCM1	25.1	40.6	

[a]The simulations correspond to the elevated CO_2 scenarios.

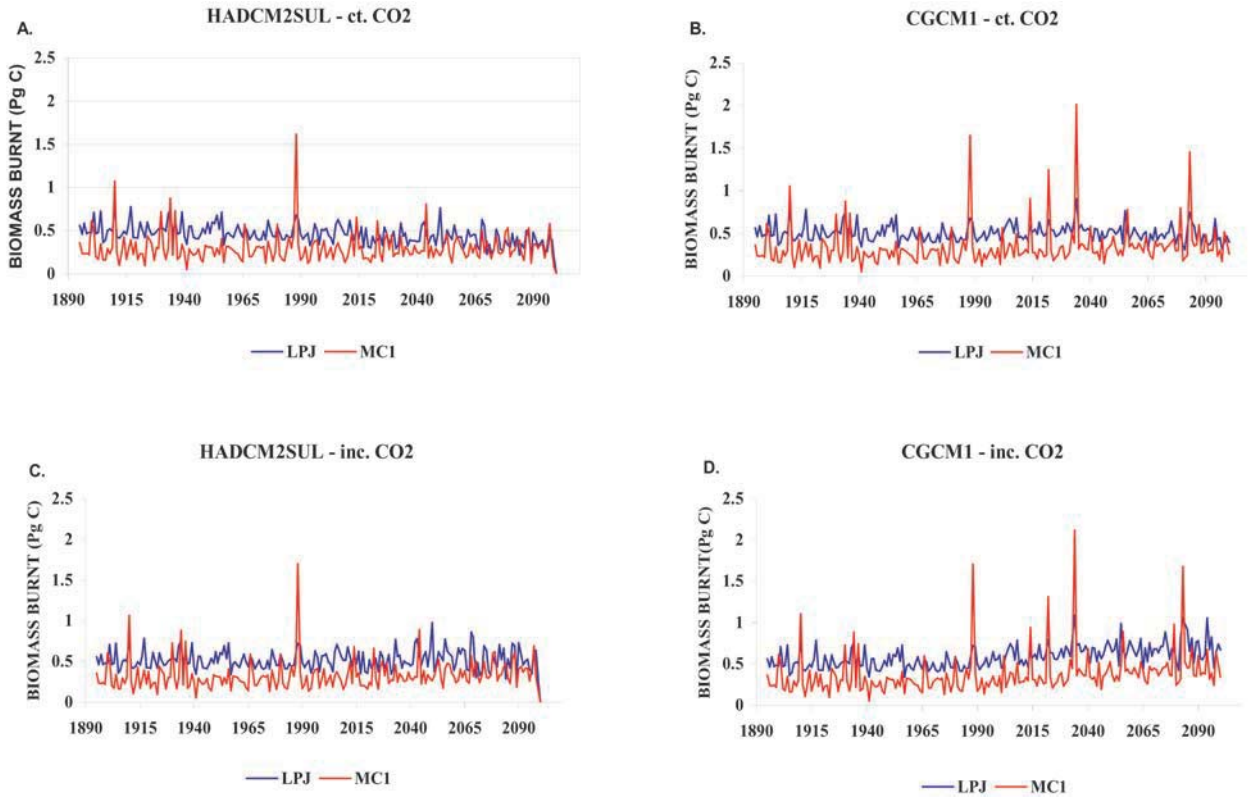

Figure 8. Total biomass consumed by fire simulated by MC1 and LPJ from 1895 to 2100 for (a, c) HADCM2SUL and (b, d) CGCM1 climate change scenarios. Models assume either a constant atmospheric CO_2 concentration of 295 ppm (ct. CO_2, and A and B) or a continuous increase in the atmospheric CO_2 concentration (inc. CO_2, C and D) from 295 ppm in 1895 to 712 ppm in 2100.

distribution and carbon cycling at broad spatial and temporal scales rather than local patterns.

6.1. Simulation Limitations

6.1.1. Climate Change Scenarios

[36] We have chosen two climate change scenarios to simulate the possible extremes in future temperature conditions. Temperatures tend to increase monotonically in both scenarios, but there is considerable interdecadal variability in precipitation. The CGCM1 scenario includes a period of decrease in precipitation early in the 21st century followed by a rapid increase at the end of the century. Only by using a variety of other scenarios would we be able to fully document the realm of possibilities in the direction of the carbon fluxes. We present in this paper a small sample of the possible outcomes and document the various ways different model structures can deal with different climate inputs.

[37] *Cox et al.* [2000] have shown that carbon-cycle feedbacks could significantly accelerate the increase in atmospheric CO_2. *Betts* [2000] showed that when forest zones are shifted northward because their historical location becomes too warm, the land surface albedo increases and enhances the release of CO_2 to the atmosphere further enhancing climate change. The increase in carbon sequestration potential due to the replacement of the tundra by forests does not necessarily compensate for the change in albedo feedback to the atmosphere. These feedbacks could not be considered in our analysis.

6.1.2. Potential Vegetation

[38] We have assumed that neither pests nor pathogens were affecting plant growth. We have also assumed no grazing and no human impacts such as agricultural development, urbanization, logging, livestock grazing, fertilization, or irrigation. Neither impacts of nitrogen deposition nor pollution were included. No extreme events such as tornadoes or floods were simulated. In the absence of disturbance other than wildfires, the impacts reported here thus refer to potential vegetation. Several authors have now documented well that the impacts of land-use changes dominate the historical C budget [e.g., *Houghton et al.*, 1999]. LPJ was used in a model comparison exercise where cropland establishment and abandonment were simulated [*McGuire*

Table 4b. Average Annual Biomass Consumed by Fire in the Conterminous United States: Simulated Versus Observed[a]

	Average Annual Biomass Consumed by Fire, Pg C		
	LPJ	MC1	*Leenhouts* [1998]
1895–1995	1.160	0.717	0.530–1.228
1994–2100: HADCM2SUL	1.155	0.796	
1994–2100: CGCM1	1.419	0.978	

[a]The simulations correspond to the elevated CO_2 scenarios.

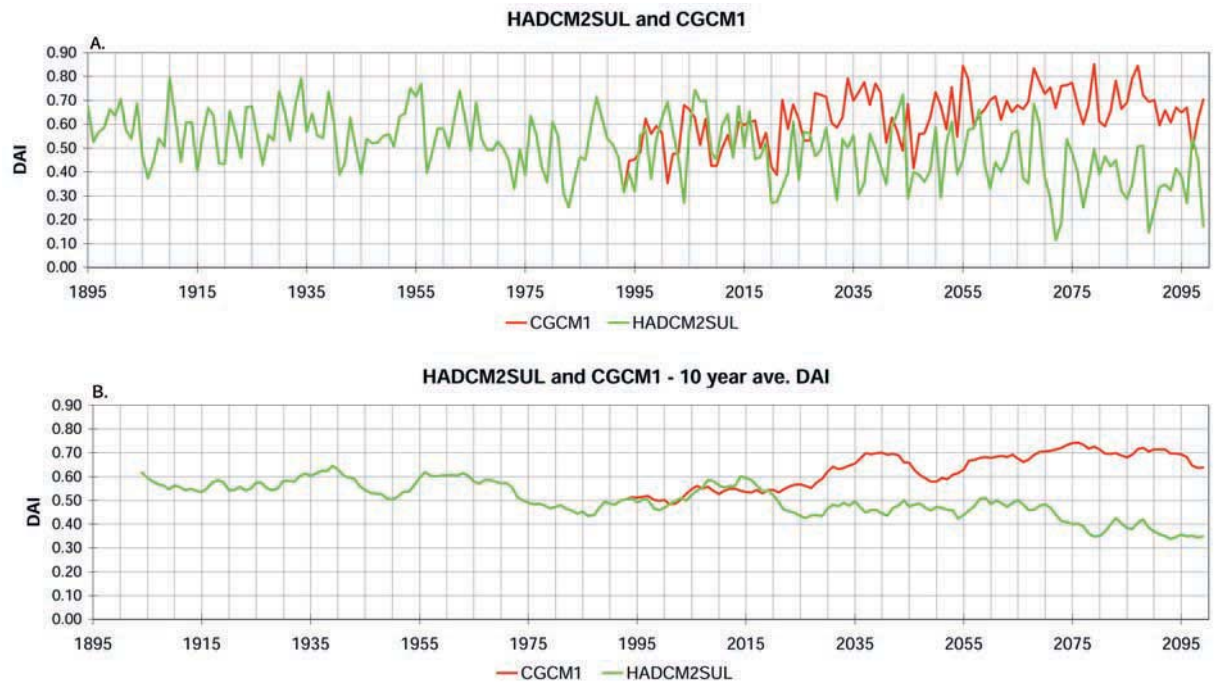

Figure 9. DAI (area of the conterminous United States where the annual Palmer Drought Severity Index is less than zero that year) under (a) HADCM2SUL and CGCM1 climate change scenarios and (b) its 10-year average.

et al., 2001]. The authors concluded that land-use change impacts were more significant than climatic changes in the last century. MC1 does not currently include the explicit impacts of agricultural and forest management practices, but the next phase of model development will include them based on the CENTURY structure.

[39] Neither LPJ nor MC1 has represented dispersal mechanisms but LPJ simulates establishment processes on bare soil. We have assumed that all vegetation types were available to grow wherever and whenever the climate permitted and that fertile soils would always be available. Furthermore, both LPJ and MC1 have assumed that there was no nutrient limitation. These assumptions were made due in large part to the lack of data that could be used to parameterize the models at the continental to global scale.

6.1.3. Validation

[40] *Küchler*'s [1964] map represents the best estimate of what the potential vegetation of the United States might be. It is difficult to compare our simulated cover types with satellite imagery or ground-truthed land-use maps because our simulations do not include human influences on the landscape and most of the United States has been heavily impacted by agriculture, forest management, and urbanization. Moreover, our simulations are dynamic with significant year-to-year variability. The frequency of fires, for example, may change the landscape composition from one year to the next, especially in the western United States, making it difficult to choose a particular year to compare it with *Küchler*'s [1964] map. We have chosen 1900 and 1990 to bracket the twentieth century and show the direction toward which changes were occurring in our simulations with regard to the published map of potential vegetation.

[41] Any error in predicting an observed vegetation type will affect the prediction of biomass and net primary production in that particular location. It would thus be unrealistic to expect regionally consistent and accurate predictions of complex ecosystem attributes like NPP. However, at the continental scale, the models should reproduce the major patterns of observed vegetation distribution and associated carbon sources and sinks.

[42] Because dynamic vegetation models simulate regional to continental scale carbon and nutrient fluxes, validation is not possible in a direct sense. Worldwide data sets are currently being gathered (e.g., S.T. Gower as cited by *Kucharik et al.* [2000], *Knapp and Smith* [2001], *Jager et al.* [2000], and the Global Primary Production Data Initiative, GPPDI) and their adequacy with respect to being scaled up to the regional scale evaluated carefully by various research teams [*Jager et al.*, 2000]. Until these data sets have been completed, modelers have to rely upon local data that may or may not be applicable to large-scale comparison. This is the reason why simple model comparisons have been used as surrogate validation exercises, since they can pinpoint weaknesses and inconsistencies between different model structures. These exercises however do not provide reliable validation [*Rastetter*, 1996]. We compared simulated NPP values from the two models with the NPP data set used by *Jager et al.* [2000] (R. J. Olson, unpublished data, 2001). Results (Table 5) show a fair agreement between model and data with weaknesses described in previous sections. We also compared model results averaged over the historical period to a set of observed data (Table 5). *Knapp and Smith* [2001] presented a set of average

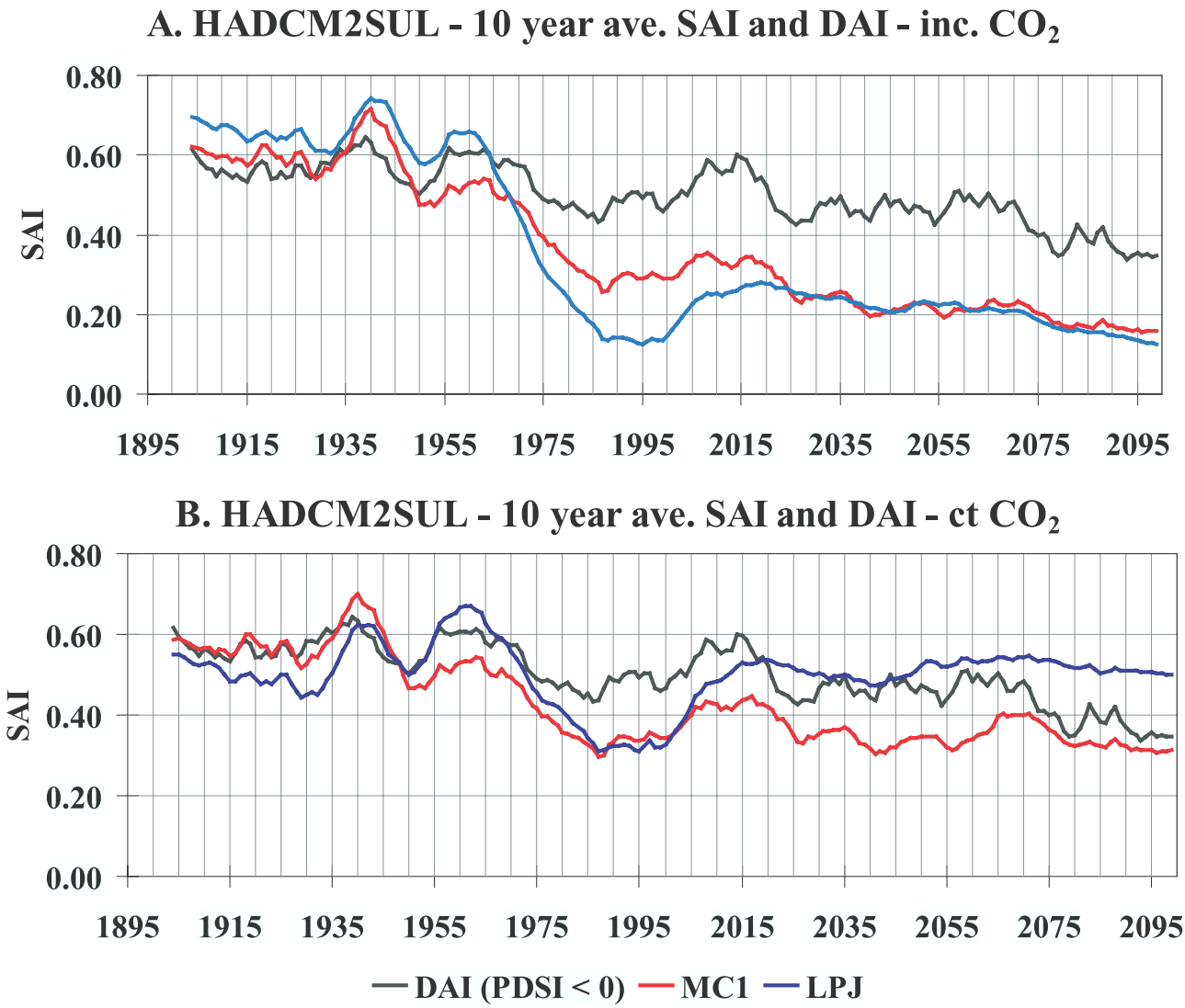

Figure 10. Percentage of the total U.S. land area under drought stress calculated using DAI or model output (LPJ and MC1) under HADCM2SUL climate change scenarios with (a) increasing or (b) constant atmospheric CO_2 concentration.

aboveground NPP values for various biomes at LTER sites across the United States. We used the ratio between ANPP and NPP presented by *Gower et al.* [1999] to estimate NPP at the LTER sites. MC1 tends to overestimate desert and savanna NPP, but in general both models agree fairly well with the observations.

6.1.4. Fire

[43] To predict and verify the impact of climate change on regional fire regimes and on the extent of the area burnt by wildfires is a difficult task complicated by the difference in scales between climate models and fire behavior and by the generalized practice of fire suppression in the United States. Fire behavior models require fine-scale environmental data, while climate change scenarios are usually provided at coarse temporal and spatial resolution. In MC1 and LPJ, monthly climatic input data are used to generate daily data to run the fire model. By doing so, using a linear interpolation, we are ignoring the potential impact of future climate on the variance of the various climate variables. The levels of biomass consumption cannot be compared to observations because the model does not include fire suppression that has been in use since before the 1930s in the United States.

[44] GCMs predict increases in temperatures that are typically associated with increased fire occurrence. However, the seasonality of these increases is important. In general, climate models project higher average winter temperatures. In areas where winters are wet, this increase will not greatly affect fire danger. However, a change in summer moisture could greatly affect fire ignition. Unfortunately, projections of monthly precipitation by the GCMs are regionally uncertain and vary greatly between models. Moreover they give no indication on potential changes in the number or duration of the storm events. More frequent El Niño-type precipitation patterns could dramatically alter the fire season.

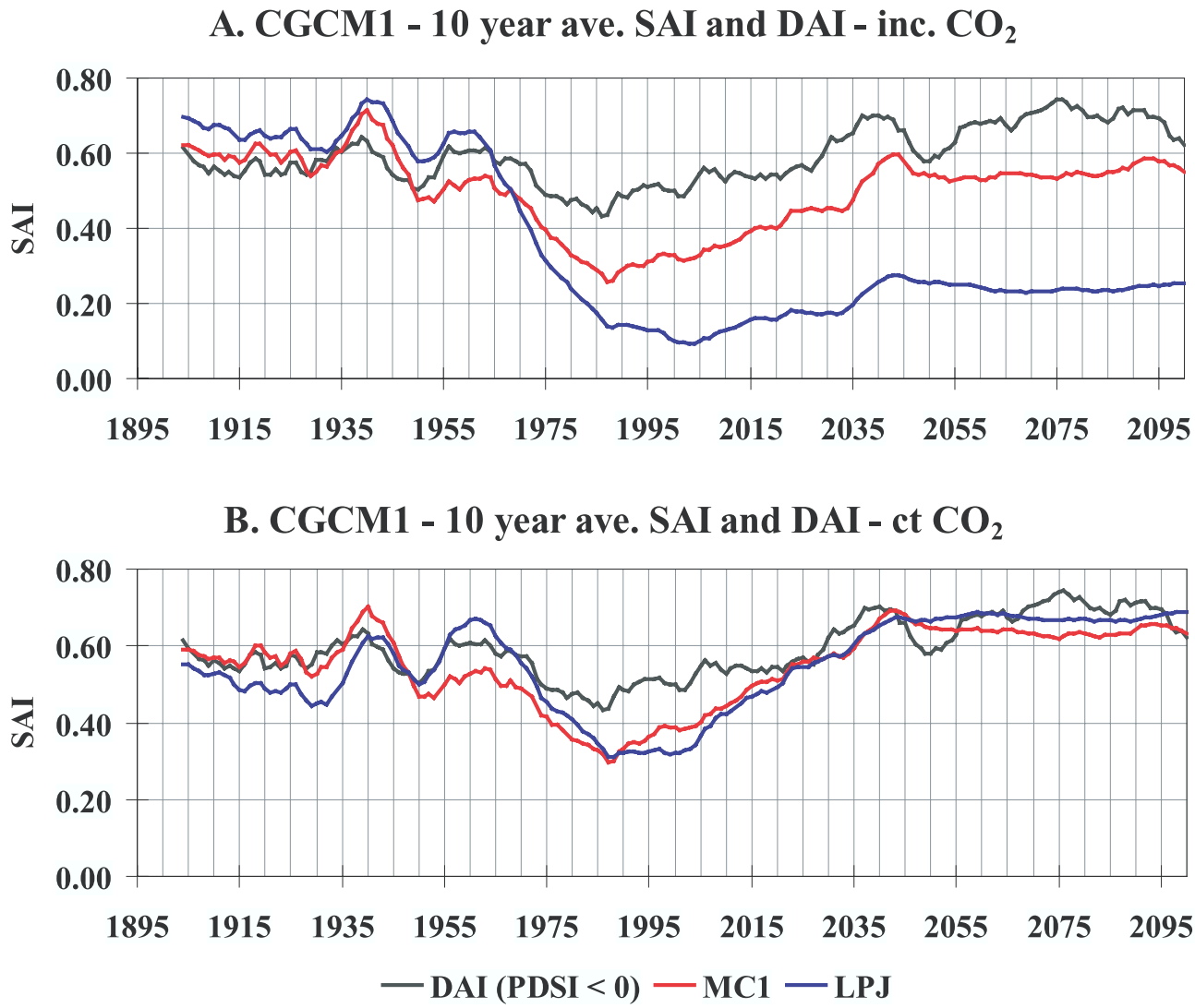

Figure 11. Percentage of the total U.S. land area under drought stress calculated using DAI or model output (LPJ and MC1) under CGCM1 climate change scenarios with (a) increasing or (b) constant atmospheric CO_2 concentration.

[45] Most of the observed large wildfires result from extreme events and have nonhomogeneous behavior responding to slope and aspect variations, wind patterns and vegetation types [*Torn and Fried*, 1992]. Extreme events are not simulated by the GCMs, and the current state of the DGVMs does not allow for explicit sub-grid cell heterogeneity. MC1 and LPJ simulate the fraction of a grid cell that is burnt using biomass and moisture characteristics that are homogeneous in the cell. Representation of fire location and timing in our simulations is thus limited and should not be interpreted as a reliable prediction. It is meant to indicate broad patterns of fire and does accurately represents high fire years such as 1910 and 1988 in the western United States.

6.2. CO_2 Sensitivity

[46] The sensitivity to CO_2 of the two models is quite different and is illustrated in the response of carbon pools and of the simulated SAIs to future conditions. Both models simulate an increase in live vegetation carbon under HADCM2SUL but only LPJ does so under CGCM1 (Figure 6). The CO_2 fertilization effect on plant production in LPJ is enough to compensate for the dry warmer climate. However, it does not compensate for soil carbon losses. Under both climate scenarios, LPJ simulates a decrease in soil C while MC1 simulates an increase under HADCM2-SUL. Thus even if the models simulate a greening up of the land, they can also simulate the depletion of the soil carbon resource that an increase in atmospheric CO_2 cannot compensate for. As we expected, both LPJ and MC1 simulate SAIs with similar dynamics to DAI under historical conditions and under future conditions when the CO_2 concentration is held constant. When the CO_2 concentration increases, the SAIs depart from the DAI trajectories as plants respond to the simulated effect of CO_2 on water use efficiency partially alleviating the negative impacts of

Table 5. Comparison Between the Average NPP Simulated by the Two DGVMs LPJ and MC1 Between 1895 and 1993 and Observed NPP From Two Sources[a]

	MC1 Mean (SD)	LPJ Mean (SD)	LTER - ANPP Mean (SE)	LTER - NPP Mean	Oak Ridge Data Set Mean (SD)
Coniferous forests	0.813 (0.077)	0.717 (0.050)			boreal: 0.318 (0.187)
					temperate maritime: 0.693 (0.282)
					temperate continental: 0.614 (0.243)
Winter deciduous forests	0.953 (0.128)	0.731 (0.080)	HF − 0.745 (0.017)	0.879	0.600 (0.276)
			HB − 0.705 (0.008)	1.268	
Mixed forests	0.963 (0.112)	0.749 (0.044)			cool temperate: 0.549 (0.116)
Savannas	0.639 (0.069)	0.494 (0.059)	CEDAR CREEK − 0.277 (0.022)	0.444	
Grasslands	0.536 (0.067)	0.332 (0.044)	KONZA − 0.443 (0.022)	0.708	tundra: 0.093 (0.064)
			CPER − 0.117 (0.010)	0.186	C3: 0.353 (0.252)
			SEV − 0.185 (0.015)	0.295	C4: 0.468 (0.239)
					arid shrub: 0.130 (0.077)
Deserts	0.233 (0.056)	0.089 (0.021)	JOR − 0.229 (0.021)	0.401	0.063 (0.043)

[a]Sources are estimated total NPP using LTER ANPP records [*Knapp and Smith*, 2001] and above to belowground production ratio calculated by *Gower et al.* [1999], mean observed NPP as collected by R. Olson (Oak Ridge National Laboratory, personal communication, 2001) and cited by *Jager et al.* [2000]. Units are Pg yr^{-1}. HF, Harvard Forest, Mass.; HB, Hubbard Brook, N. H.; CEDAR CREEK, Cedar Creek, Minn.; KONZA, Konza Prairie, Kans.; CPER, Central Plains Experimental Range, Colo.; SEV, Sevilleta, N. M.; JOR, Jornada, N. M.

droughts. The models disagree with the magnitude of that effect under CGCM1.

[47] The difference between the model responses can be explained by the different ways the CO_2 effect is implemented in the two models. Elevated CO_2 influences vegetation growth through enhanced photosynthesis [*Farquhar et al.*, 1980], and indirectly through reduced water use [*Drake et al.*, 1997; *Farquhar*, 1997]. In LPJ, both effects are simulated mechanistically. The direct effect is included in the modified Farquhar photosynthesis scheme [*Collatz et al.*, 1991, 1992] that is adopted to calculate gross photosynthesis. The indirect effect is implemented through the dynamic feedback between photosynthesis and soil hydrology through canopy conductance. The indirect CO_2 effect becomes particularly important under conditions of water stress. When the simulated transpirational water demand exceeds the supply of water, canopy conductance and photosynthesis are reduced until supply and demand are balanced. For a given canopy conductance, a higher intercellular CO_2 concentration can be maintained if atmospheric CO_2 is elevated, increasing the Rubisco-limited rate of photosynthesis. Water use efficiency increases consequently and renders the vegetation more drought tolerant. This is clearly illustrated by the low SAI simulated by LPJ under the drier CGCM1 scenario (Figure 11) in comparison with that simulated by MC1 where the CO_2 effect is not as effective. In MC1, scalars are used to increase gross primary production and C:N ratios which control production and death rates. These scalars increase production nonlinearly by up to 25% when atmospheric CO_2 concentration reaches 700 ppm. Potential evapotranspiration is decreased by another nonlinear scalar that also reaches 25% at 700 ppm.

[48] The magnitude of the CO_2 fertilization effect is still debated [e.g., *Prentice et al.*, 2001]. LPJ has been applied to simulate the CO_2 fertilization effect at the Duke Forest Free Air CO_2 Enrichment (FACE) experiment [*DeLucia et al.*, 1999] that is the first replicated long-term FACE study in an intact forest ecosystem. The simulated productivity enhancement due to continuous CO_2 elevation by 200 ppm was in the same range as observed (T. Hickler et al., Elevated CO_2 and productivity at the Duke Forest FACE experiment: A test of the LPJ model, submitted to *Global Ecology and Biogeography*, 2002). Because of the positive effect of elevated CO_2 on water use efficiency, LPJ also correctly predicted the highest CO_2 effect in 1998, which was a severe drought year. But the model did not simulate the observed decline of the response from the fourth year onward observed at the FACE prototype [*Oren et al.*, 2001], which presumably was caused by nutrient limitations, mainly nitrogen [*Oren et al.*, 2001]. However, the generality of these results remains to be tested. It is likely that the constraint on CO_2 fertilization by nutrient availability differs among environments and ecosystem types. *Casperson et al.* [2000] showed no evidence of any growth enhancement from CO_2 fertilization in various forests along a latitudinal gradient in the eastern United States from 1930 to 1980. Given the importance of simulating CO_2-induced carbon uptake for future projections, much work remains to be done to establish the credentials of ecosystem models in this field.

6.3. Fire Effects

[49] LPJ and MC1 fire modules are fundamentally similar in that they both simulate a fraction of the cell area burnt as some function of fuel moisture and fuel loading. But they differ significantly in the level of detail used to simulate these fuel characteristics and their effect on fire severity. The MC1 fire module simulates fire behavior (e.g., fire spread, fire intensity, crown versus surface fire) as a link between environmental drivers (maximum temperature, relative humidity, precipitation, soil moisture) and fire effects (fuel consumption, root mortality, cambial kill), in contrast to the more empirical approach of the LPJ module where fire effects (fuel consumption) are a more direct function of the environment (soil moisture). Simulating fire behavior in MC1 requires more extensive linkage between the fire functions and the dynamic biogeography and biogeochemical functions than is necessary in LPJ. Including the fire behavior produces a fire module more sensitive to extreme conditions of climate and fuels. The result is a more

dynamic MC1 simulation of biomass consumed by fire characterized by infrequent events of extreme severity that are largely absent from the LPJ simulation. Differences in the average annual biomass consumed simulated by the two fire modules (Table 4b) are mostly due to the fact that LPJ simulates higher vegetation biomass (Figures 5c and 5d) than MC1. But it is also related to the MC1 fire behavior. In MC1, fire effects are partitioned between live biomass mortality and live and dead biomass consumption, partly as a function of fire behavior. Biomass killed but not consumed is transferred to dead biomass pools. In LPJ, there is no provision for mortality without consumption, so all fire-effected biomass is consumed. If biomass mortality is added to biomass consumed by fire, the total amount of fire-effected biomass simulated by MC1 is nearly equal to the biomass consumed by fire in LPJ. Because fire enhances litter inputs to the soil in MC1, soil carbon simulated by MC1 remains more stable under warmer and drier conditions (CGCM1) than in the LPJ simulation (Figures 5e and 5f), thus keeping the carbon sequestration potential an option for mitigation of increasing CO_2 in the future.

6.4. Conclusions

[50] Vegetation changes under a warm and dry climate scenario such as CGCM1 can appear quite startling and may stretch the believability of the results. However, recent discoveries of rapid changes in interdecadal climate regimes bolster the credibility of the dramatic climatic shifts occurring over 1–3 decades such as under CGCM1. The Pacific Decadal Oscillation (PDO) changed in the mid-1970s [*Karl*, 1998], reversing a 30-year trend of cooling to one of warming. The previous shift from warming to cooling occurred around 1940. Both shifts were accompanied by extreme weather events [*Neilson*, 1986]. Another phase shift in the PDO may be under way, indicated in part, by a dramatic shift in salmon runs in the Pacific Northwest [*Mantua et al.*, 1997, 1999]. Paleoecological records also indicate that extreme climates have occurred in the past, over periods of decades to centuries [*National Research Council*, 2002]. In the VEMAP scenario, CGCM1 simulates a decline in precipitation of about 4% by the 2030s followed by a shift to a dramatic increase in precipitation reaching about 22% by 2100. Much of the simulated future decline in precipitation occurs in the southeast while much of the increased precipitation occurs in the west. We believe these results are within the realm of possible future climate shifts.

[51] The next questions are then: How rapidly can the vegetation respond to this rapid climate change and are the models accurately capturing the possible rates of vegetation change? Forest decline and dieback can occur quite rapidly under persistent or extreme drought stress. The drought of 1988 produced considerable forest dieback in both eastern and western United States [*Changnon*, 1989; *Riebsame et al.*, 1991]. The drought of the early 1950s produced a large dieback of woodlands and savannas in the Southwest with some reorganization of ecotones [*Allen and Breshears*, 1998]. Under CGCM1, both LPJ and MC1 suggest a rapid, drought-induced decline in southeastern forests, indicated by a reduction in vegetation density. Such a shift from a forest to possibly a savanna requires only the loss of trees and could occur over a period of years to decades. A shift in species composition would only likely occur over a longer timespan.

[52] Expansion of species into new areas or shifts in the dominance of existing lifeforms are difficult phenomena to predict accurately. Since our models do not simulate species but lifeforms, the issue of migration rate cannot be addressed. However, recent analyses suggest that the rate of migration of species would be quite slow compared to climate change [*Davis and Zabinski*, 1992]. Over the next 100 years, many species may not move beyond the bounds we have set for a single simulation grid cell (50 km) whereas some of the model results suggest movements of lifeforms over several hundred kilometers. Shifts in lifeform dominance are most likely the initial response to climatic shifts. Most ecosystems contain many lifeforms, for example, occasional broadleaf trees within conifer forests, or persistent few shrubs within grasslands. Climate shifts could allow these comparatively rare lifeforms to become dominant. Successional processes will likely be governed by changes in the competitive balance within the context of a shifting climate. Local dispersal will constrain how rapidly a relatively rare lifeform can spread within a local ecosystem. Gap-phase succession could govern some of these rates, modulated in part by the rate of gap creation, as well as local dispersal [*Shugart*, 1984]. Gap creation would be in part a function of whether the climate change is relatively benign, for example, to warmer and wetter conditions, or whether it is stressful, such as to warmer and drier conditions, accompanied by fire, insects, or diseases. Neither MC1 nor LPJ simulates local competitive and dispersal rate processes, nor do they include insects or diseases. Thus their results must be taken as indications of the direction and possible rate of change since considerable uncertainty remains in the rapidity of shifts in lifeform dominance. On a longer timescale, these shifts would be accompanied by long-distance dispersal and a gradual change in species composition. Accurate simulation of the latter process would require a better understanding of dispersal, establishment, and competitive interactions of newly arriving species into existing, possibly quite healthy ecosystems. These are research challenges for the future.

[53] The rate of vegetation change will also be affected by the extent of the CO_2 fertilization effect. However, it is still uncertain to what extent the positive effect of CO_2 on photosynthesis and water-use efficiency (WUE) [*Long et al.*, 1996; *Will and Teskey*, 1997; *Curtis and Wang*, 1998; *Saxe et al.*, 1998] diminishes when resources such as water and nitrogen become limiting. Increased WUE has often been associated with a reduction in stomatal conductance. The apparent lack of stomatal response in a Free Air CO_2 Exchange (FACE) experiment at the Duke experimental forest has raised concerns that the WUE effect might not materialize [*Ellsworth*, 1999]. However, increased WUE is a direct function of the counter-exchange of CO_2 and water molecules through the stomata. Their ratio will increase regardless of stomatal conductance, simply as a function of increased external CO_2 concentration. Thus elevated CO_2 could confer to plants some measure of drought resistance as soil water becomes limiting. Clearly, however, photo-

synthesis will still be curtailed as water stress increases. How much drought resistance elevated CO_2 will confer is still a matter of some uncertainty. MC1 uses a simple empirical function for both fertilization and WUE effects while LPJ uses a more process-based approach following Farquhar photosynthesis theory. The more process-based approach is probably more accurate but is also the most sensitive of the two approaches. Neither approach has yet been fully tested and implementation of even the best theories requires the incorporation of some assumptions. Thus the two models can be viewed as representing the possible bounds of responses by vegetation to increased CO_2 concentration.

[54] The two models which adopted widely different approaches to model ecosystem dynamics consistently simulated similar overall trends in past and future dynamics of natural ecosystems throughout the conterminous United States. Both models agree that desert areas would be greatly reduced under both scenarios by the end of the 21st century and that the eastern deciduous forests would expand westward at the expense of the central grasslands. More generally, both models simulate that moderate warming such as that projected under HADCM2SUL would contribute to an increase in plant growth as atmospheric CO_2 concentration is increasing while additional warming would cause droughts and carbon release to the atmosphere potentially enhancing climate change through positive feedbacks. Under increasing atmospheric CO_2, both models simulate increases in NPP between historical and future climatic conditions (except for mixed forests simulated by MC1). Under constant CO_2, both models simulate decreases in forest NPP (except for coniferous forests simulated by LPJ). Both models simulate an increase in the number of large fires under the warmer and drier CGCM1 scenario. Both models simulate a decrease in soil carbon storage under the warmer climate scenario CGCM1 but only MC1 simulates a slight increase in soil C storage under moderate warming. This means that even if vegetation growth is enhanced by increasing atmospheric CO_2 concentration and warm temperatures, decomposition may also be enhanced and thus prevent C accumulation and sequestration in the soil. The stress area index confirms this idea and shows that plants can counteract the drought impacts to a certain extent but that above a certain threshold [*Bachelet et al.*, 2001b], drought conditions prevail and carbon losses are to be expected. Uncertainty in modeling results is commonly assessed by using several models. This is useless if all the models share the same assumptions. For a few key features in our two models, such as the ecosystem response to increasing CO_2, it is still uncertain which model representation is more realistic. As long as such uncertainties persist, model comparisons used to project future vegetation dynamics should include a variety of approaches.

[55] While several authors [*Schimel et al.*, 2000; *Houghton et al.*, 1999] have emphasized the role of land use changes in the carbon budget of the United States, this paper illustrates the fact that natural vegetation dynamics governed by natural disturbance such as wildfires can also affect carbon fluxes significantly. As the vegetation responds to changes in climate and in the resulting shifts in fire regime, changes in plant distribution and their density affect both the productivity of the site and the soil response to those changes. Sequestration potential depends in large part on the inputs to the soil and the decomposition flora and fauna. When the dominant lifeform changes, it affects soil processes and modifies the overall carbon, nutrient, and water budget of the site. Moreover, after a disturbance such as fire, decomposition and nutrient release or immobilization will depend on the production of new litter and the reestablishment of the decomposing organisms. While we completely recognize the essential role played by human impacts through land use changes, we also want to emphasize the essential role of the vegetation dynamics for which fire is a key driver and emphasize the need for a better handle on succession processes. MC1 and LPJ are the only DGVMs that simulate wildfires mechanistically. Most of the models that have been used to calculate global or regional carbon budgets [*Potter and Klooster*, 1999; *Schimel et al.*, 2000] include fixed vegetation distribution and prescribed fire regimes. By modifying the distribution of the vegetation as a response to climatic variability and resulting fire regimes, MC1 and LPJ brush a new picture of possible trends in carbon fluxes that have not been discussed before.

[56] **Acknowledgments.** The authors want to thank Tim Kittel and the VEMAP Data group at NCAR (Boulder, Colorado) for providing us with the climate scenarios, and David Yates from the Research Application Program, NCAR (Boulder, Colorado), for providing us with PDSI data. They also want to thank Steve Wondzell and two anonymous reviewers for their helpful comments on the manuscript. This work was funded in part by the U.S. Department of Energy, National Institute for Global Environmental Change, Great Plains Region (LWT 62-123-06509); the U.S. Geological Survey, Biological Resources Division, Global Change Program (CA-1268-1-9014-10); and the USDA-Forest Service, PNW, NE, SE Stations (PNW 95-0730). The Lund group acknowledges with thanks the financial support for VEMAP provided by the Electric Power Research Institute (EPRI), Palo Alto, California.

References

Allen, C. D., and D. D. Breshears, Drought-induced shift of a forest woodland ecotone: Rapid landscape response to climate variation, *Proc. Natl. Acad. Sci. USA*, *95*, 14,839–14,842, 1998.

Bachelet, D., J. Lenihan, C. Daly, and R. Neilson, Interactions between fire, grazing and climate change at Wind Cave National Park, SD, *Ecol. Modell.*, *134*, 224–229, 2000.

Bachelet, D., J. Lenihan, C. Daly, R. Neilson, D. Ojima, and W. Parton, MC1: A dynamic vegetation model for estimating the distribution of vegetation and associated ecosystem fluxes of carbon, nutrients, and water, *Pac. Northwest Stn. Gen. Tech. Rep. PNW-GTR-508*, 95 pp., U.S.D.A. For. Serv., Washington, D. C., 2001a.

Bachelet, D., R. P. Neilson, J. M. Lenihan, and R. J. Drapek, Climate change effects on vegetation distribution and carbon budget in the U.S., *Ecosystems*, *4*, 164–185, 2001b.

Betts, R. A., Offset of the potential carbon sink from boreal forestation by decreases in surface albedo, *Nature*, *408*, 187–190, 2000.

Boer, G. J., G. M. Flato, M. C. Reader, and D. Ramsden, A transient climate change simulation with historical and projected greenhouse gas and aerosol forcing: experimental design and comparison with the instrumental record for the 20th century, *Clim. Dyn.*, *16*, 405–425, 1999a.

Boer, G. J., G. M. Flato, and D. Ramsden, A transient climate change simulation with historical and projected greenhouse gas and aerosol forcing: Projected climate for the 21st century, *Clim. Dyn.*, *16*, 427–450, 1999b.

Brovkin, V., A. Ganopolski, and Y. Svirezhev, A continuous climate-vegetation classification for use in climate-biosphere studies, *Ecol. Modell.*, *101*, 251–261, 1997.

Casperson, J. P., S. W. Pacala, J. C. Jenkins, G. C. Hutt, P. R. Moorcroft, and R. A. Birdsey, Contributions of land-use history to carbon accumulation in forests, U.S., *Science*, *290*, 1148, 2000.

Changnon, S. A., The 1988 drought, barges, and diversion, *Bull. Am. Meteorol. Soc.*, *70*, 1092–1104, 1989.

Collatz, G. J., J. T. Ball, C. Grivet, and J. A. Berry, Physiological and environmental regulation of stomatal conductance, photosynthesis and transpiration: A model that includes a laminar boundary layer, *Agric. For. Meteorol.*, *54*, 107–136, 1991.

Collatz, G. J., J. T. Ball, C. Grivet, and J. A. Berry, Coupled photosynthesis-stomatal conductance model for leaves of C_4 plants, *Austral. J. Plant Physiol.*, *19*, 519–538, 1992.

Cox, P., R. Betts, C. Jones, S. Spall, and I. Totterdell, Acceleration of global warming due to carbon-cycle feedbacks in a coupled climate model, *Nature*, *408*, 184–187, 2000.

Cramer, W., et al., Global response of terrestrial ecosystem structure and function to CO_2 and climate change: Results from six dynamic global vegetation models, *Global Change Biol.*, *7*, 357–373, 2001.

Curtis, P. S., and X. S. Wang, A meta-analysis of elevated CO_2 effects on woody plant mass, form, and physiology, *Oecologia*, *113*, 299–313, 1998.

Daly, C., D. Bachelet, J. M. Lenihan, R. P. Neilson, W. Parton, and D. Ojima, Dynamic simulation of tree-grass interactions for global change studies, *Ecol. Appl.*, *10*, 449–469, 2000.

Davis, M. B., and C. Zabinski, Changes in geographical range resulting from greenhouse warming: Effects on biodiversity in forests, in *Global Warming and Biological Diversity*, edited by R. L. Peters and T. E. Lovejoy, pp. 297–308, Yale Univ. Press, New Haven, Conn., 1992.

DeLucia, E. H., et al., Net primary production of a forest ecosystem with experimental CO_2 enrichment, *Science*, *284*, 1177–1179, 1999.

Diaz, H. F., Some aspects of major dry and wet periods in the contiguous United States, 1895–1981, *J. Clim. Appl. Meteorol.*, *22*, 3–16, 1983.

Drake, B. G., M. A. Gonzales-Meler, and S. P. Long, More efficient plants: A consequence of rising atmospheric CO_2?, *Annu. Rev. Plant Physiol. Plant Mol. Biol.*, *48*, 609–639, 1997.

Ellsworth, D. S., CO_2 enrichment in a maturing pine forest: Are CO_2 exchange and water status in the canopy affected, *Plant Cell Environ.*, *22*, 461–472, 1999.

Farquhar, G. D., Carbon dioxide and vegetation, *Science*, *278*, 1411, 1997.

Farquhar, G. D., S. von Caemmerer, and J. A. Berry, A biochemical model of photosynthetic CO_2 assimilation in leaves of C3 plants, *Planta*, *149*, 78–90, 1980.

Flato, G. M., G. J. Boer, W. G. Lee, N. A. McFarlane, D. Ramsden, M. C. Reader, and A. J. Weaver, The Canadian Center for Climate Modelling and Analysis Global Coupled Model and its climate, *Clim. Dyn.*, *16*, 451–467, 1999.

Foley, J. A., I. C. Prentice, N. Ramankutty, S. Levis, D. Pollard, S. Sitch, and A. Haxeltine, An integrated biosphere model of land surface processes, terrestrial carbon balance, and vegetation dynamics, *Global Biogeochem. Cycles*, *10*, 603–628, 1996.

Friend, A. D., and A. White, Evaluation and analysis of a dynamic terrestrial ecosystem model under preindustrial conditions at the global scale, *Global Biogeochem. Cycles*, *14*, 1173–1190, 2000.

Friend, A. D., A. K. Stevens, R. G. Knox, and M. G. R. Cannell, A process-based, terrestrial biosphere model of ecosystem dynamics (Hybrid v3.0), *Ecol. Modell.*, *95*, 249–287, 1997.

Gower, S. T., C. J. Kucharik, and J. M. Norman, Direct and indirect estimation of leaf area index, f_{apar}, and net primary production of terrestrial ecosystems, *Remote Sens. Environ.*, *70*, 29–51, 1999.

Haxeltine, A., and I. C. Prentice, A general model for the light-use efficiency of primary production, *Funct. Ecol.*, *10*, 551–561, 1996a.

Haxeltine, A., and I. C. Prentice, BIOME3: An equilibrium terrestrial biosphere model based on ecophysical constraints, resource availability, and competition among plant functional types, *Global Biogeochem. Cycles*, *10*, 693–709, 1996b.

Haxeltine, A., I. C. Prentice, and I. D. Creswell, A coupled carbon and water flux model to predict vegetation structure, *J. Veg. Sci.*, *7*, 651–666, 1996.

Houghton, R. A., J. L. Hacker, and K. T. Lawrence, The U.S. carbon budget: Contributions from land-use change, *Science*, *285*, 574–578, 1999.

Jager, H. I., W. W. Hargrove, C. C. Brandt, A. W. King, R. J. Olson, J. M. O. Scurlock, and K. A. Rose, Constructive contrasts between modeled and measured climate responses over a regional scale, *Ecosystems*, *3*, 396–411, 2000.

Jarvis, P. G., and K. G. McNaughton, Stomatal control of transpiration: Scaling up from leaf to region, *Adv. Ecol. Res.*, *15*, 1–49, 1986.

Johns, T. C., R. E. Carnell, J. F. Crossley, J. M. Gregory, J. F. B. Mitchell, C. A. Senior, S. F. B. Tett, and R. A. Wood, The second Hadley Center coupled ocean-atmosphere GCM: Model description, spinup and validation, *Clim. Dyn.*, *13*, 103–134, 1997.

Karl, T. R., Regional trends and variations of temperature and precipitation, in *The Regional Impacts of Climate Change: An Assessment of Vulnerability*, edited by R. T. Watson et al., pp. 412–425, Cambridge Univ. Press, New York, 1998.

Kattenberg, A., et al., Climate models-Projections of future climate, in *Climate Change 1995: The Science of Climate Change: Contribution of Working Group 1 to the Second Assessment Report of the Intergovernmental Panel on Climate Change*, edited by J. T. Houghton et al., pp. 285–357, Cambridge Univ. Press, New York, 1996.

Kirilenko, A. P., and A. M. Solomon, Modeling dynamic vegetation response to rapid climate change using bioclimatic classification, *Clim. Change*, *38*, 15–49, 1998.

Knapp, A. K., and M. D. Smith, Variation among biomes in temporal dynamics of aboveground primary production, *Science*, *291*, 481–484, 2001.

Kucharik, C. J., J. A. Foley, C. Delire, V. A. Fisher, M. T. Coe, J. D. Lenters, C. Young-Molling, and N. Ramankutty, Testing the performance of a dynamic global ecosystem model: Water balance, carbon balance, and vegetation structure, *Global Biogeochem. Cycles*, *14*, 795–825, 2000.

Küchler, A. W., Potential natural vegetation of the conterminous United States, manual to accompany the map, *Spec. Publ. 3*, 143 pp., Am. Geogr. Soc., New York, 1964.

Leenhouts, B., Assessment of biomass burning in the conterminous United States, *Conserv. Ecol.*, *2*, 1, 1998. (Available at http://www.consecol.org/vol2/iss1/art1)

Lenihan, J. M., C. Daly, D. Bachelet, and R. P. Neilson, Simulating broad-scale fire severity in dynamic global vegetation model, *Northwest Sci.*, *72*, 91–103, 1998.

Linacre, E. T., A simple formula for estimating evaporation rates in various climates, using temperature data alone, *Agric. Meteorol.*, *18*, 409–424, 1977.

Long, S. P., C. P. Osborne, and S. W. Humphries, Photosynthesis, rising atmospheric carbon dioxide concentration and climate change, in *Global Change Effects on Coniferous Forests and Grasslands*, edited by A. I. Breymeyer et al., pp. 121–159, John Wiley, New York, 1996.

Mantua, N. J., S. R. Hare, Y. Zhang, J. M. Wallace, and R. C. Francis, A Pacific interdecadal climate oscillation with impacts on salmon production, *Bull. Am. Meteorol. Soc.*, *78*, 1069–1079, 1997.

Mantua, N. J., P. dell'Arciprete, and R. C. Francis, Patterns of climate variability in the PNW: A regional 20th century perspective, in *Impacts of Climate Variability and Climate Change in the Pacific Northwest: An Integrated Assessment*, edited by E. D. Miles, report, 110 pp., Pac. Northwest Reg. Assess. Group for the U.S. Global Change Res. Program, Clim. Impacts Group, Univ. of Wash., Seattle, 1999.

McGuire, A. D., et al., Carbon balance of the terrestrial biosphere in the twentieth century: Analyses of CO_2, climate and land use effects with four process-based ecosystem models, *Global Biogeochem. Cycles*, *15*, 182–206, 2001.

Mitchell, J. F. B., and T. C. Johns, On modification of global warming by sulfate aerosols, *J. Clim.*, *10*, 245–267, 1997.

Monteith, J. L., Accommodation between transpiring vegetation and the convective boundary layer, *J. Hydrol.*, *166*, 251–263, 1995.

National Research Council, *Abrupt Climate Change: Inevitable Surprises*, Natl. Acad., Washington, D. C., 2002.

Neilson, R. P., High-resolution climatic analysis and southwest biogeography, *Science*, *232*, 27–34, 1986.

Neilson, R. P., A model for predicting continental-scale vegetation distribution and water balance, *Ecol. Appl.*, *5*, 362–385, 1995.

Nigam, S., M. Barlow, and E. H. Berbery, Analysis links Pacific decadal variability to drought and streamflow in the United States, *Eos Trans. R. Soc. AGU*, *80*, 621–625, 1999.

Oren, R., et al., Soil fertility limits carbon sequestration by forest ecosystems in a CO_2-enriched atmosphere, *Nature*, *411*, 469–472, 2001.

Palmer, W. C., Meteorological drought, *Res. Pap. 45*, 58 pp., U.S. Weather Bur., Washington, D. C., 1965.

Pan, Y., et al., Modeled responses of terrestrial ecosystems to elevated atmospheric CO_2: A comparison of simulations by the biogeochemistry models of the Vegetation/Ecosystem Modeling and Analysis Project (VEMAP), *Oecologia*, *114*, 389–404, 1998.

Parton, W. J., D. S. Schimel, C. V. Cole, and D. Ojima, Analysis of factors controlling soil organic levels of grasslands in the Great Plains, *Soil Sci. Soc. Am.*, *51*, 1173–1179, 1987.

Parton, W. J., et al., Observations and modeling of biomass and soil organic matter dynamics for the grassland biome worldwide, *Global Biogeochem. Cycles*, *7*, 785–809, 1993.

Potter, C. S., and S. A. Klooster, Detecting a terrestrial biosphere sink for carbon dioxide: Interannual ecosystem modeling for the mid-1980s, *Clim. Change*, *42*, 489–503, 1999.

Prentice, I. C., et al., The carbon cycle and atmospheric carbon dioxide, in *Climate Change 2001: The Science of Climate Change: Contribution of Working Group I to the Third Assessment Report of the Intergovernmental Panel on Climate Change*, edited by J. T. Houghton et al., pp. 183–239, Cambridge Univ. Press, New York, 2001.

Rastetter, E. B., Validating models of ecosystem response to global change, *Bioscience*, *46*, 190–198, 1996.

Riebsame, W. E., S. A. Changnon, and T. R. Karl, *Drought and Natural Resources Management in the United States: Impacts and Implications of the 1987–1989 Drought*, pp. 11–92, Westview, Boulder, Colo., 1991.

Rothermel, R. E., A mathematical model for predicting fire spread in wildland fuels, *Res. Pap. INT-115*, 40 pp., U.S.D.A. For. Serv., Intermt. For. and Range Exper. Stn., Washington, D. C., 1972.

Saxe, H., D. S. Ellsworth, and J. Heath, Tree and forest functioning in an enriched CO_2 atmosphere, *New Phytol.*, *139*, 395–436, 1998.

Schimel, D., and B. H. Braswell, Continental scale variability in ecosystem processes: Models, data, and the role of disturbance, *Ecol. Monogr.*, *67*, 251–271, 1997.

Schimel, D., et al., Contribution of increasing CO_2 and climate to carbon storage by ecosystems in the United States, *Science*, *287*, 2004–2006, 2000.

Shugart, H. H., *A Theory of Forest Dynamics*, Springer-Verlag, New York, 1984.

Sitch, S., The role of vegetation dynamics in the control of atmospheric CO_2 content, doctoral dissertation, Inst. of Ecol., Plant Ecol., Lund Univ., Lund, Sweden, 2000.

Sitch, S., et al., Evaluation of ecosystem dynamics, plant geography and terrestrial carbon cycling in the LPJ Dynamic Global Vegetation Model, *Global Change Biol.*, *9*, 161–185, 2003.

Smith, B., I. C. Prentice, and M. T. Sykes, Representation of vegetation dynamics in the modelling of terrestrial ecosystems: Comparing two contrasting approaches within European climate space, *Global Ecol. and Biogeogr.*, *10*, 621–638, 2001.

Thonicke, K., S. Venevsky, S. Sitch, and W. Cramer, The role of fire disturbance for global vegetation dynamics: Coupling fire into a Dynamic Global Vegetation Model, *Global Ecol. Biogeogr.*, *10*, 661–677, 2001.

Torn, M., and J. S. Fried, Predicting the impacts of global warming on wildland fire, *Clim. Change*, *21*, 257–274, 1992.

Will, R. E., and R. O. Teskey, Effect of irradiance and vapor-pressure deficit on stomatal response to CO_2 enrichment of four tree species, *J. Exper. Bot.*, *48*, 2095–2102, 1997.

Woodward, F. I., M. R. Lomas, and R. A. Betts, Vegetation-climate feedbacks in a greenhouse world, *Philos. Trans. R. Soc. London, Ser. B*, *353*, 29–38, 1998.

D. Bachelet, Oregon State University, Forestry Sciences Laboratory, 3200 SW Jefferson Way, Corvallis, OR 97331, USA. (bachelet@fsl.orst.edu)

R. J. Drapek, J. M. Lenihan, and R. P. Neilson, Forestry Sciences Laboratory, U.S. Forest Service, 3200 SW Jefferson Way, Corvallis, OR 97331, USA. (rdrapek@fs.fed.us; jlenihan@fs.fed.us; rneilson@fs.fed.us)

T. Hickler, B. Smith, and M. T. Sykes, Climate Impacts Group, Department of Physical Geography and Ecosystems Analysis, University of Lund, Sölvegatan 13, S-223 62 Lund, Sweden. (Thomas.hickler@planteco.lu.se; Ben.Smith@planteco.lu.se; martin@planteco.lu.se)

S. Sitch and K. Thonicke, Potsdam Institute for Climate Impact Research, Telegrafenberg C4, P.O. Box 60.12.03, 14412 Potsdam, Germany. (Stephen.sitch@pik-potsdam.de; kirsten@pik-potsdam.de)